A STUDY OF PRG4 AS IT RELATES TO URIC ACID AND GOUT

By

Talia D'Ambruoso

Bioengineering BS, The University of Massachusetts: Dartmouth, 2017

Thesis

Submitted in partial fulfillment of the requirements for the Degree of Master of Science in the Graduate Program of Biomedical Engineering at Brown University

PROVIDENCE, RHODE ISLAND

February 2022

AUTHORIZATION TO LEND AND REPRODUCE THE THESIS

As the sole author of this thesis, I authorize Brown University to lend it to other institutions for the purpose of scholarly research.

Date_____ _____
TALIA D'AMBRUOSO, Author

I further authorize Brown University to reproduce this thesis by photocopying or other means, in total or in part, at the request of other institutions or individuals for the purpose of scholarly research.

Date_____ _____
TALIA D'AMBRUOSO, Author

This thesis by Talia D'Ambruoso is accepted in its present form by the Center for Biomedical Engineering as satisfying the thesis requirements for the degree of Master of Science

Date_____ Signature: _____

Dr. GREGORY JAY, Advisor

Date_____ Signature: _____

Dr. MARISSA GRAY, Reader

Date_____ Signature: _____

Dr. BRADEN FLEMING, Reader

Approved by the Graduate Council

Date_____ Signature: _____

Dr. Andrew G. Campbell, Dean of the Graduate School

Acknowledgements

I'd like to thank Dr. Gregory Jay and Dr. Ling Zhang, for their knowledge and instrumental guidance in completing this work. Without their willingness to instruct, this would not have been possible.

I'd also like to thank all those at Brown University that I have worked with for the mentorship and direction received throughout pursing this degree.

Lastly, I wish to thank those at RI Hospital and the Lifespan system that have enabled my learning and provided practical training.

Table of Contents

Table of Figures

Table of Tables

Abstract of A STUDY OF PRG4 AS IT RELATES TO URIC ACID AND GOUT, by Talia D'Ambruoso, ScM, Brown University, DECEMBER, 2021.

Objective: Proteoglycan-4 (PRG4) is a mucinous glycoprotein expressed by synovial fibroblasts and plays an important role in joint heath. The objective of thesis was to identify a new mechanism of action by PRG4 as it relates to gout and uric acid.

Methods: MSU crystal growth studies were conducted comparing rhPRG4 to bovine submaxillary mucin (BSM) as a comparator., CXCL and IL1β ELISA studies in macrophages from *Prg4*$^{-/-}$ mice, and conditional knockout mice gait analysis methods were completed. Gait analysis in *Prg4*$^{-/-}$ mice and knee joint friction studies are ongoing for osteoarthritis investigation.

Results: PRG4 suppresses MSU crystal growth (average 8 crystals at 96 hrs, 100 mcg/ml) as compared to BSM (average 231 crystals at 96 hrs, 100 mcg/ml). Also, pre-formed MSU crystals biofouled with rhPRG4 suppress CXCL and IL1β expression. In vivo, Prg4 conditional mice injected with MSU crystals in the presence (swing time, 0.0795 s) and absence (swing time, 0.0468 s) of lubricin production showed detectable differences in gait analysis.

Conclusions: These data are important due to the rising cases of gout and the necessity for alternative treatments in both acute and chronic cases. Future work will focus on understanding the mechanism of action between PRG4 and MSU crystal formation.

Chapter 1: Introduction

Gout is a chronic inflammatory arthritic disease characterized by monosodium urate crystal (MSU) deposition mainly in and around joint tissue. Gout typically presents as acute onset of pain in the lower limbs, specifically the metatarsophalangeal joint and peaks within 24 hours followed by resolution within 7-14 days. MSU crystals form due to increased serum uric acid (SUA), known as hyperuricemia and occur when the concentration is in excess of 6.8 mg/dL. Increased SUA can be caused by several factors but ultimately is due to an imbalance in purine production or intake compared to excretion from the kidneys and the gastrointestinal tract. The first potential cause of increased SUA is the overproduction of UA due to enzyme deficiencies, such as Lesch-Nyham syndrome and super activity of phosphoribosyl pyrophosphate synthetase (Ragab, 2017). Diet high in purine and alcohol consumption are the major sources of increase in SUA. Accelerated cell turnover can also increase endogenous production, and is most frequently due to malignancies, hematological and inflammatory diseases, chemotherapy, and tissue damage (Ragab, 2017).

Gout: A Manifestation of Hyperuricemia

Urate is excreted via renal (60-65%) or extra-renal routes of elimination (35-40%). Renal excretion includes filtration in the kidneys via the glomerulus, then passes into the proximal tube where reabsorption and secretion take place. This is measured as fractional excretion of urate, FEUA = excreted urate/filtered urate. Extra-renal elimination takes places in the intestines, with urate entering via secretion into the bloodstream, or as a component of bile, saliva, or peptic juices, and is reabsorbed in the intestine and finally excreted in feces (Hyndman, 2016) (Hosomi, 2012).

Figure 1.

Pathogenesis of hyperuricemia (perceived and designed by Dr. EL-Shahaly) (Ragab, 2017)

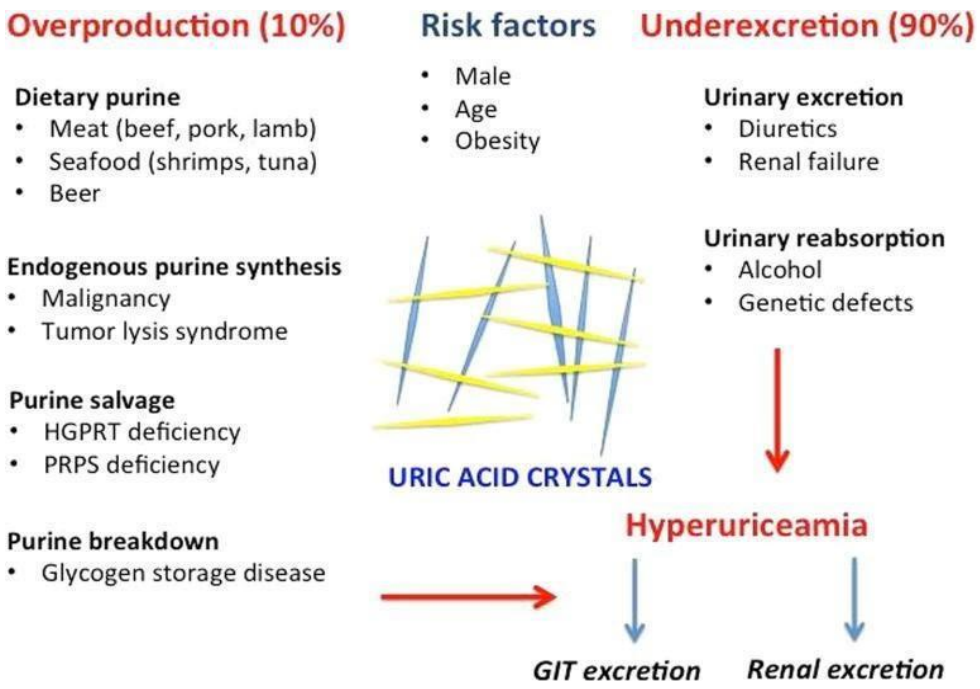

Legend: This figure depicts the sources of urate acid intake and pathway for excretion in patients with history of gout and hyperuricemia.

MSU crystal deposition into joint tissue causes an inflammatory response. This starts with the activation of monocytes and mast cells, then further promulgated by neutrophils. Macrophages engulf the MSU crystals and produce TNF, IL-1, IL-6 and IL-8 and concomitant paracrine endothelial cell activation including chemokines, following the phagocytosis (Busso, 2010). These chemokines predominantly include IL-8 (CXCL8) and GROα (CXCL1) which are largely responsible for neutrophil recruitment (Busso, 2010).

Gout is present in four stages: asymptomatic hyperuricemia, acute gouty attack, inter-critical period, and chronic tophaceous gout (Ragab, 2017). Asymptomatic hyperuricemia is a period of no symptoms of gout. An acute gouty attack is the characteristic monoarthritic peak within a severely inflamed joint that

shows redness, warmth, tenderness, swelling, or loss of function with a range of time between attacks (Grassi, 2012). The inter-critical period is when the attack dissipates and symptoms resolve, typically after treatment. Chronic tophaceous gout results from repetitive gouty attacks and typically progresses to joint destruction, damaging the joint surfaces, and causes formation of palpable tophi (large crystal accumulation in soft tissues) (Ragab, 2017).

Figure 2.

Pathogenesis of acute gouty inflammation (Ragab, 2017)

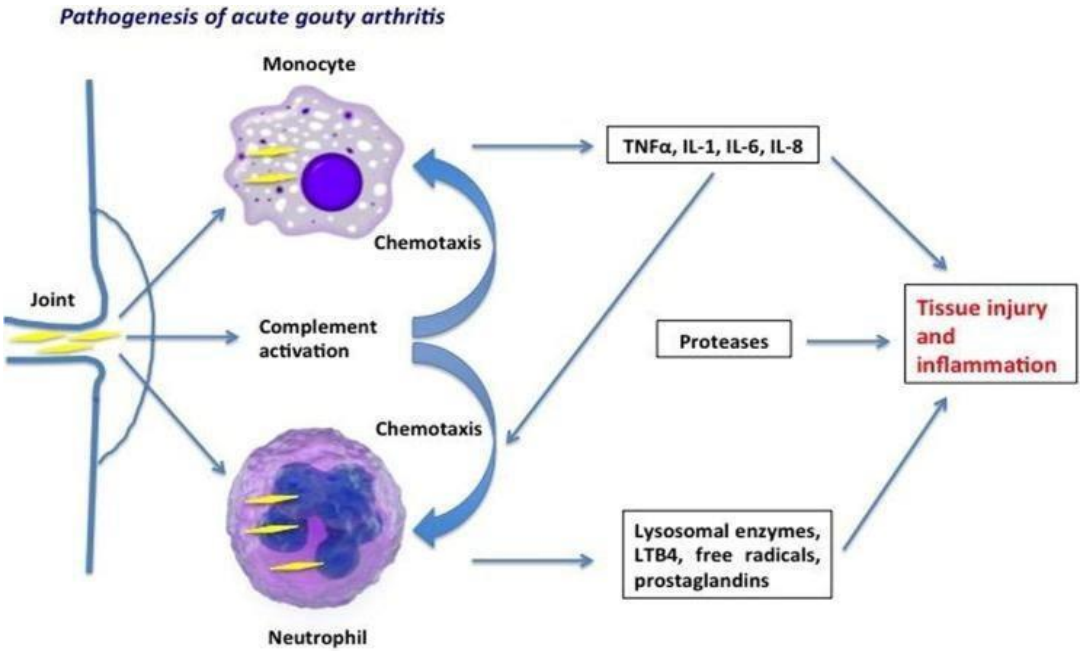

Legend: This figure depicts how the process when MSU crystals initiate the inflammatory response in an acute gouty attack.

Gout is diagnosed through visualization and identification of the MSU crystal in the synovial fluid. Imaging techniques such as conventional radiography, CT, dual-energy CT, MRI, PET, and ultrasound are commonly used for diagnosis and treatment (Parathithasan, 2016). The articular cartilage 'double contour sign' (DCS) observed ultrasonographically is specific for gout and is an abnormal hyperechoic band over the superficial margin of the articular hyaline cartilage (Ragab, 2017).

Figure 3.

MSU crystal deposition (Towiwat, 2019)

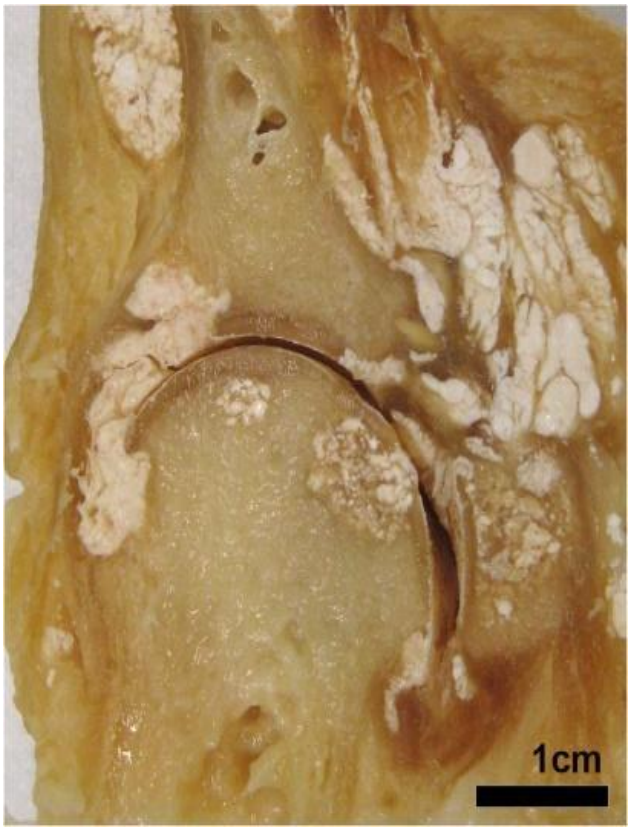

Legend: This figure shows MSU crystal deposition in in the left first metatarsophalangeal joint, along with tophus and joint damage.

Clinical Management of Gout

Gout is a manageable disease and can be treated with pharmacological therapy. Pharmacological therapy in acute gout includes nonsteroidal anti-inflammatory drugs (NSAIDS), corticosteroids, and colchicine. Xanthine oxidase inhibitors (XOI) or uricosuric drugs, such as allopurinol, can be used for recurrent or severe disease after the acute attack has passed. These above treatment methods are used for the treatment of an acute gouty attack and can relieve symptoms within 24 hours (Dalal, 2020). While cost prohibitive, IL-1 inhibitors are a new potential treatment for gout, with anakinra, rilonacept, and canakinumab currently in clinical trials (Schlesinger, 2014). Nonpharmacological therapy includes patient

education, dietary selection, weight loss, and resting the joint. Opioids are commonly used in the treatment and management of acute gout flare ups. In one study 28.3% of patients with an average dose of 37.9 ± 17.2SD mg of morphine equivalent for a median duration of 8 days (interquartile range 5–14), received opioids at discharge from the emergency department (Dalal, 2020). Given the increase in prevalence of gout, now as common as rheumatoid arthritis, and the desire to avoid opioids when possible (47,600 opioid overdose deaths in US 2017), there is interest in alternative treatments in managing the acute gouty attack and preventative methods (Wilson, 2020) (Dehlin, 2020).

Uric acid is a by-product of purine nucleotide breakdown, and at normal physiological conditions of pH 7.4 and 37°C, urate circulates in plasma and synovial fluid in mono-deprotonated ionic form (Martillo, 2013). The most frequent form of MSU crystal formation in gout is monosodium monohydrate $NaC_5H_3N_4O_3 \cdot H_2O$. These crystals have triclinic structure (faces on three unequal axes non perpendicular to the others) and are macroscopically visible as needle structures. The crystals are formed when sheets purine rings with urate anions hydrogen-bond together, then continue to stack together. These MSU crystals form in supersaturated solution, above 6.8 mg/dl urate concentration (Martillo, 2013).

Figure 4.

Uric Acid Physical Chemistry (Martillo, 2013)

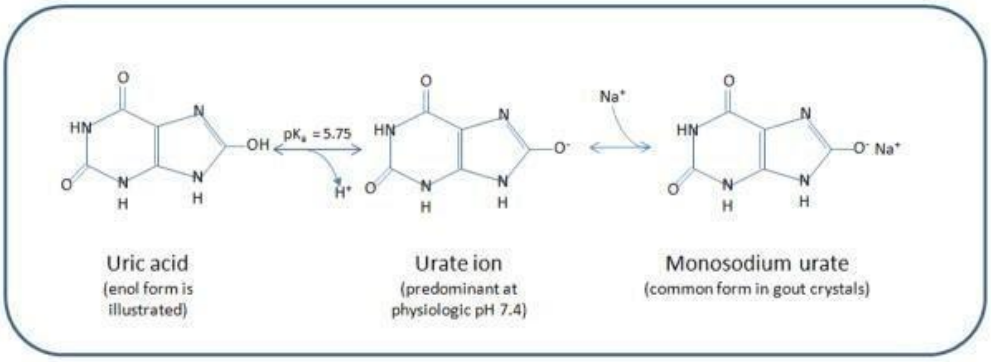

Legend: This image shows the uric acid and monosodium urate physical chemistry. It is the sheets of purine rings that stacks upon itself to produce a needle shaped structure.

The MSU crystal formation increases when the crystals coagulate together and form crystal nuclei, with individual crystals growing in length. Decreased temperature and acidic conditions will increase crystal formation, which is a primary reason why the metatarsophalangeal joint, a peripheral joint, is a frequent gouty attack location (Martillo, 2012).

Role of PRG4 in Gout

Lubricin is a mucinous glycoprotein secreted in the synovial joint that provides boundary lubrication to protect the joint. It is expressed by the gene Proteoglycan-4 (PRG4), more so in the superficial but also intermediate zone chondrocytes and by synoviocytes (Jay, 2014). Boundary lubrication functions during high load and low entraining velocity when the lubricating layer is thinner than the surface roughness (Waller, 2013). The protein has a central mucin domain with a repeating motif of KEPAPTT that is O-linked with β(1-3)-Gal-GalNAc glycosylation, and globular N- and C-termini. The N-terminus creates a disulphide bond to link adjacent lubricin monomers. Both the N- and C-termini interact with the cartilage surface (Jay, 2014).

Lubricin has been demonstrated to act as a chondroprotective agent in multiple animal models, including rat meniscectomy and ACL transection models (Vugmeyster, 2012) (Jay, 2012). In patients with ACL rupture and established osteoarthritis (OA) there have been diminished levels of lubricin in the synovial fluid (Elsaid, 2009). Patients that do not properly express or have functional protein develop Camptodactyly-arthropathy-coxa vara-pericarditis (CACP) (Choi, 2004). This is an autosomal recessive disorder and causes early joint failure associated with non-inflammatory synoviocytes hyperplasia and subintimal fibrosis of the synovial capsule (Jay, 2014).

One hypothesis for initiation of OA is an increase in coefficient of friction due to loss of boundary lubricant in synovial fluid due to the proteolytic degradation of PRG4 as a result of the post-injurious

inflammatory response (Jay, 2012). This increase in the coefficient of friction leads to increased shear stress at the cartilage surface which impacts chondrocyte metabolic function and survival and leads to edge-stage OA (Waller, 2013).

In addition to its well known lubricating roles, PRG4 has an anti-inflammatory effect mediated by its interaction with surface receptor CD44, which antagonizes TLR2 and TLR4 (Alquraini, 2015). This was evaluated by in the past co-incubating MSU crystals ± rhPRG4 or bovine submaxillary mucin (BSM), to measure crystal phagocytosis, cytokine and chemokine expression. rhPRG4 reduced NFκB nuclear translocation, NLRP3 expression, caspase-1 activation and generation of mature IL-1β ($p < 0.05$) (Quadri, 2018). The anti-inflammatory properties from PRG4 occur because it competes with hyaluronan on binding with the CD44 receptor. Binding with CD44 inhibits IL-1β and TNF-α induced NFκB nuclear translocation in synoviocytes from patients with RA and OA (Qadri, 2018). Binding with CD44 also results in entry of PRG4 into the cell where it interacts with and inhibits the NLRP3 inflammasome (Qadri, 2018).

Figure 5.

Lubricin Structure on Surface (Jay, 2014)

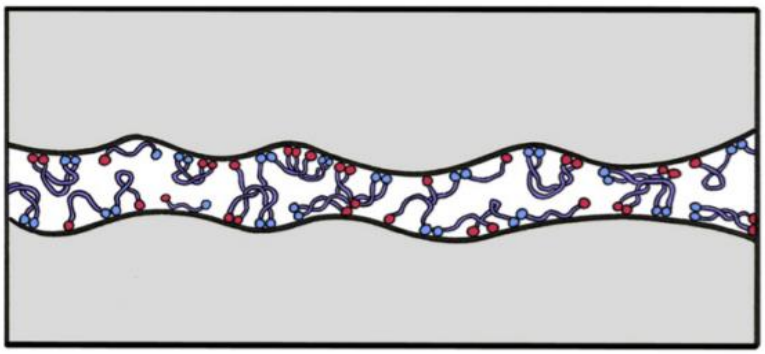

Legend: This diagram shows the lubricin glycoprotein structure on apposed cartilage surfaces.

Antifreeze Glycoproteins: A Natural Model of O-linked β(1-3)-Gal-GalNAc on a Repeating Protein Motif

Antifreeze proteins (AFPs) and antifreeze glycoproteins (AFGPs) have been identified as a body fluid constituent of polar fish species which enable survival in subzero temperature waters; colder than the equilibrium freezing point of their blood and bodily fluids. There are four structures of AFP (type I, II, II, IV) and one class of AFGPs. These proteins suppress seed ice crystal growth within the fish bodily fluid (Harding, 2003).

Figure 6.

Classification of antifreeze glycoproteins proteins (Harding, 2003).

Characteristic	AFGP	Type I AFP	Type II AFP	Type III AFP	Type IV AFP
Mass (Da)	2600 – 33000	3300 – 4500	11000 – 24000	6500	12000
Key Properties	AAT repeat; disaccharide	Alanine-rich α-helix	Disulfide bonded	β-sandwich	Alanine rich; helical bundle
Representative Structure	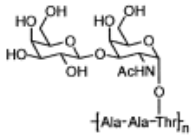				
Natural Source	Antarctic notothenioids; northern cods	Right-eyed flounders; sculpins	Sea raven; smelt; herring	Ocean pout; wolfish; eel pout	Longhorn sculpin

Legend: This diagram describes the type of antifreeze glycoproteins and key primary and secondary structure information for each.

There are at least eight structurally similar glycoproteins that make up the class of AFGP known today. All have repeating units of $(Ala\text{-}Ala\text{-}Thr)_n$, with minor sequence variation and the disaccharide β-d-galactosyl-(1→3)-α-N-acetyl-d-galactosamine joined as a glycoside to the hydroxyl oxygen (O-linked) of the Thr residues. They also vary in molecular mass from 33.7 kDA to 2.6 kDA. This variation is present and identified in a range of polar fish with AFGP (Harding, 2003). AFGP exhibit thermal hysteresis,

which is determined by measurement of kinetic ice growth point and subtraction of the freezing point of a solution. The freezing point is proportional to the molar fraction of molecules in solution, and the growth of seed ice crystals is much greater than this. Higher molecular mass AFGP exhibit more thermal hysteresis properties at lower concentrations than the lower molecular mass of AFGP proteins (Harding, 2003).

A secondary mechanism of suppressing ice seed crystal growth that AFGP contributes to is through modification of the crystal formation process. AFGP has been shown to create hexagonal pits on the exposed surface of ice and once fully covered, the ice growth stops (Harding, 2003).

The solution conformation of AFGPs has been studied using CD, Raman spectroscopy, light scattering measurements, and NMR spectroscopy (Harding, 2003). AFGP has a partially flexible, random coil conformation with a left-handed 3-residue-per-turn helix. The protein remains in a relatively similar structure when in the presence of ice and in a freeze-dried state (Harding, 2003).

Hypothesis: rhPRG4 Prevents MSU Crystallization

This study investigated the ability of rhPRG4 to inhibit to growth of MSU crystals from a saturated uric acid solution, and secondarily the interaction between rhPRG4 and pre-formed crystals and whether rhPRG4 would block the inflammation pathways *in vitro* in macrophages harvested from mice. Mutant mouse models, with conditional Prg4 expression, also received intra-articular MSU crystals *in vivo* to demonstrate the anti-inflammatory effects of mice expressing Prg4 compared to animals that did not. These studies required technical skills in gait analysis acquired in this thesis from other related studies. Gait was used objectively to observe and understand lameness initiated by intra-articular MSU in the presence and absence of PRG4. Proficiency in conducting these experiments was acquired in determining the impact of re-establishing Prg4 expression in a mutant mouse model following the intra-articular delivery of a helper dependent virus that expresses Prg4. In that effort animal gait was assessed via

DigiGait gait analysis of *Prg4*$^{-/-}$mice that received a helper dependent virus (HDV) that expresses Prg4 (HDV-*Prg4*) or HDV-empty, provided the opportunity to iteratively measure quadruped gait in a novel animal model. Other work was also conducted using knee joint friction pendulum techniques. This work is relevant to osteoarthritis as a potential treatment to prevent cartilage deterioration in genetic or acquired lubricin deficiency in patients (Waller, 2013).

Chapter 2: Methods

Studies for MSU and rhPRG4 interaction as it relates to gout are detailed below.

Sources of Biologicals: rhPRG4 is a full-length product produced by CHO-M cells, molecular mass is approximately 240 KDa (Lubris, Framingham, MA, USA) (Alquraini, 2015). Bovine Submaxillary Mucin (BSM; molecular mass > 1000 KDa) (Sigma Aldrich, St Louis, MO).

Regulatory Approval: All animal studies were approved by the RIH Animal Welfare Committee. Animal euthanasia methods are compliant with the American Veterinary Medical Association 2020 Guidelines (U.S. Department of Health and Human Services, n.d.).

Methods related to gout:

1. MSU Crystal Growth Studies with BSM & rhPRG4
    1. Outline: Evaluate MSU crystal quantify and length in the presence of various concentrations of rhPRG4 and BSM over 24hour intervals.
    2. Relevance: We hypothesize that rhPRG4 may inhibit MSU crystal growth in quantity and length and use BSM to compare.

Figure 7.

Crystal Growth Method

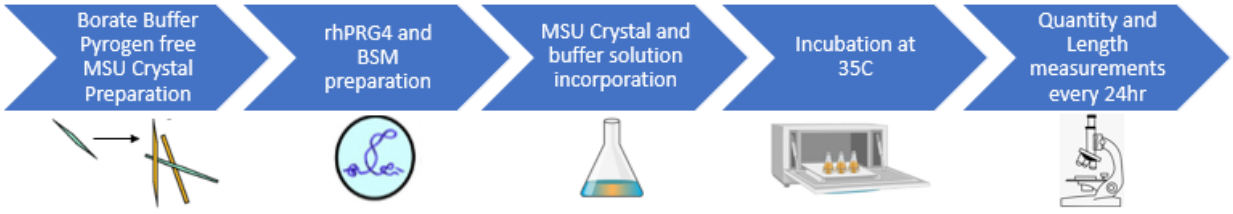

Legend: This figure describes the method summary for the crystal growth studies.

2. MSU & *Prg4*$^{-/-}$ Cell Macrophage ELISA Testing

1. Outline: Evaluate effect of rhPRG4 biofouled MSU crystals for IL1β and CXCL expression via ELISA testing.
2. Relevance: We hypothesize that rhPRG4 may inhibit MSU crystal induced IL1β and CXCL expression in murine macrophages (Qadri, 2016).

Figure 8.

ELISA Testing Method

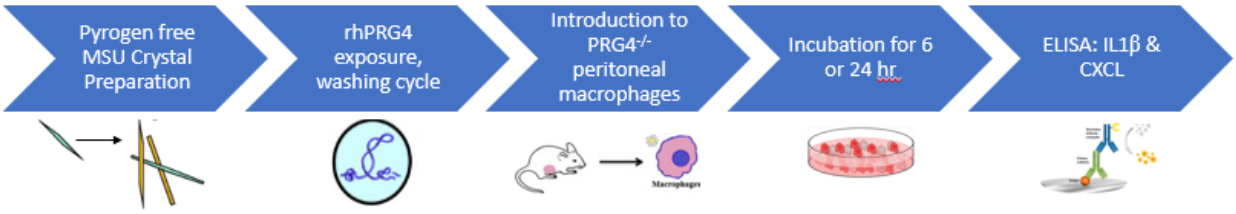

Legend: This diagram describes the method summary for the IL1β and CXCL study.

3. DigiGait Mouse Analysis - MSU crystal injected Prg4 conditional mice
    1. Outline: Prg4 conditional knockout mice ($Prg4^{CreERt2/+}$) were injected with tamoxifen, PBS, or sham injection at 4 weeks of age. 8 weeks later mice were injected in both hind legs with MSU crystals and underwent gait analysis.
    2. Relevance: This study provides data assessing the effect of MSU crystals following IA injection on gait analysis when lubricin is and is not expressed.

Method Specific Protocols:

MSU Crystal Growth Studies in BSM & rhPRG4

1. Uric acid & rhPRG4 solution preparation

50ml of 0.1M borate buffer (8.5pH, sodium tetraborate boric acid) was incubated in water bath at 37°C for T=10 min. 75 mg of uric acid (Sigma Aldrich, St. Louis MO) was measured and added to the borate

buffer solution, mixed and incubated again in a water bath for t=10 min. 1ml centrifuge tubes were labeled per the desired rhPRG4 and BSM concentrations (0, 6.25, 12.5, 25, 50, 100, 150, 200, and 250mcg/ml). Concentrations of rhPRG4 and BSM were calculated and added to the 1ml centrifuge tubes, with required additional PBS and 800ul of borate buffer uric acid solution. The solutions were created in triplicate and incubated at 35°C for t=96 hours and measured at each 24 hour interval. The table below shows the specific rhPRG4, PBS, and uric acid amounts per each concentration. The uric acid concentration in borate buffer was identified by iteratively and gradually increasing the concentration of uric acid until a clear and non-precipitating solution was observed at 37°C.

Table 1. Solution Calculations

Test Group Concentration (µl/ml)	BSM or rhPRG4 (µl)	PBS (µl)	Uric Borate solution (µl)	Test solution (µl)
0	0	200	800	1000
6.2	3.1	196.8	800	1000
12.5	6.2	193.7	800	1000
25	12.5	187.5	800	1000
50	25	175	800	1000
100	50	150	800	1000
150	75	125	800	1000
200	100	100	800	1000
250	125	75	800	1000

2. Crystal count & length measurement

At 24hour intervals, the number of MSU crystals formed were counted under 10x magnification with a hemocytometer. 20-25ul of solution was collected from the same samples each day for measurements, the 1ml tubes were mixed with a vortex for 10-20 sections prior to collection. Measurements were taken in triplicate and included crystal quantity, longest crystal length in the center cell of the hemocytometer, and images. Images were taken for each set of measurements and displayed based on highest image quality and image presence. Prism was used for statistical analysis.

MSU & *Prg4*$^{-/-}$ Macrophage ELISA Testing

1. Animal dissection & cell collection

Prg4$^{-/-}$ and wild type littermates of both sexes were euthanized. Murine peritoneal macrophages harvesting was adapted from Zhang et al, 2008. Briefly, the abdomen of each mouse was soaked with 70% alcohol and a small incision was made along the midline with scissors. Using blunt dissection, the abdominal skin was retracted to expose the intact peritoneal wall. A 27 G needle attached to a 10ml syringe filled with sterile PBS at 4°C was inserted through the peritoneal wall at the midline and injected into each mouse, aspirated slowly from the peritoneum, and the peritoneal macrophages were collected and kept on ice.

2. Cells are collected through centrifugation

The collected PBS peritoneal macrophages were centrifuged for 10min at 10,000rpm. Cell culture medium, RPMI1640 (RPMI with 10% RBS, 1% penicillin/streptomycin) (Thermo Fisher Scientific, Waltham, MA) was warmed to 37°C in preparation.

3. Cell Counting

The excess fluid from the centrifuged cells was carefully discarded, and 3ml RPMI media was added to each large tube and mixed with a pipette multiple times. In a 1ml centrifuge tube, 50ul trypsin blue stain and 50ul mixed cell culture media from the large centrifuge tube was added. Cells were counted under magnification with a hemocytometer, then the small centrifuge tubes were discarded. To large centrifuge tubes, media was added to total 19ml/tube. The cell concentration was counted for each group and typically achieved a concentration of $1.3x10^6$ cells.

4. Cells are plated into slides, incubated for 24hours at 37C, 5%CO_2

N=3 sterile chamber slide (Millipore, Tullagreen, Carrigtwohill, Co. Cork, IRL) plates were labeled for each animal group as animal group, C (control), MSU (MSU crystals; Invivogen, USA), or ML (MSU

crystals and rhPRG4, molecular mass is approximately 240 KDa). 1ml of cell solution to N=3 wells was added to each chamber slide. The slides were incubated for T=24hours at 37°C 5% CO_2.

5. MSU crystals and MSU crystals + rhPRG4 are added per test group, and incubated for 6 or 24 hours

4ml rhPRG4 and 360ul MSU crystals (MSU, InvivoGen) were combined and incubated for 2 hours at 35°C, then stored at 4°C. The rhPRG4 and MSU crystal solution was added to ML groups at concentration of 0.2mg/ml (ML group is rhPRG4 and MSU together), and MSU crystals were added to MSU groups at concentration of 0.1mg/ml. The chamber slides were incubated again for T=6 or T=24 hours at 37°C 5% CO_2. The MSU and ML groups had the same final concentration of MSU crystals.

6. After time, slide media & cells are collected for ELISA at stored at 4C

After each time point, T=6 and t=24hours, the cell solution from each well was collected for the ELISA testing and stored at 4C. The slides were then washed with 1x PBS then fixed with 4% formalin for 10 min. After washing, the slides were permeabilized with 0.1% TritonX-100 for 10 min. After washing 3 times, the slides were mounted with DAPI mounting medium (Vector Labs, Burlingame, CA) and stored at room temperature until imaging.

DigiGait Mouse Analysis - MSU crystal injected *Prg4* conditional mice

1. Mice Preparation

Prg$^{-/-}$ conditional knockout mice (PRG4$^{CreERt2/+}$) were injected with tamoxifen, PBS, or sham injection at 4 weeks of age. 8 weeks later, the animals were injected in both hind limbs with MSU crystals. The animals were allowed to convalesce for 24 hrs with no limitation in ambulation then underwent gait analysis and were then euthanized followed by knee joint fixation in formaldehyde for future histology.

2. Gait Processing

The DigiGait software was opened, the specific study folder was selected, then the individual data files for processing (shown as @ status) were selected. The boundary box for each mouse file was confirmed and re-drawn as needed, then the paw image was filtered to eliminate noise in the data. The software was advanced until graphical gait data was shown. The specific graphs were assessed and filtered to eliminate any overlapping data points or inaccurate data. The files were exported as .csv as needed once completed.

Methods related to Animal Models:

The methods and techniques used in the above study were informed by an earlier effort using HDV-EF1-*Prg4* IA injected *Prg4*$^{-/-}$ mice which was an attempt to convert the *Prg4* null mouse into a Prg4 expressing animal. Methods are illustrated below and data from that effort has been included in the Appendix.

1. DigiGait Mouse Analysis - HDV-*Prg4* Injection in Prg4 Null Mice (RIH IACUC approval: Quadruped Gait and Regulation of Apoptotic Factors in Tibiofemoral Joints Following Intra-Articular HDV-*Prg4* Injection in Prg4 Null Mice: An Emerging Treatment for CACP in Humans)
    1. Outline: 4-week-old *Prg4*$^{-/-}$ mice were injected with IA HDV-EFI-*PRG4* and HDV-empty, along with wild type mice and control mice, for gait alteration study at post-injection weeks t=0, 2, 4, and 6 weeks.
    2. Relevance: *Prg4*$^{-/-}$ mice function as an arthrosis model to understand joint failure attributable to lack of lubrication and to understand the pathogenesis of osteoarthritis where low levels of PRG4 have been found. Gait modification due to osteoarthritis has been previously characterized and hypothesized to have relevance in this study (Emad, 2013).

Method Specific Protocols:

DigiGait Mouse Analysis - HDV-*Prg4* Injection in *Prg4*$^{-/-}$ Mice

1. Mice Preparation

4-week-old *Prg4*$^{-/-}$ mice were injected with IA HDV-EFI-*Prg4* and HDV-EF1-empty, along with wild type mice and control mice (*Prg4*$^{-/-}$ mice, no HDV injection), for gait alteration study at post-injection weeks t=0, 2, 4, and 6 weeks.

2. DigiGait Processing

The DigiGait software was opened, the specific study folder was selected, then the individual data files for processing (shown as @ status) were selected. The boundary box for each mouse file was confirmed and re-drawn as needed, then the paw image was filtered to eliminate noise in the data. The software was advanced until graphical gait data was shown. The specific graphs were assessed and filtered to eliminate any overlapping data points or inaccurate data. The files were exported as .csv as needed once completed.

Chapter 3: Results

The results for each study are outlined below.

MSU Crystal Growth Studies in BSM & rhPRG4

Figure 9.

MSU crystal growth images for BSM & rhPRG4

	Time (hr)			
Concentration	24	48	72	96
0ug/ml (PBS)	 507 2.05	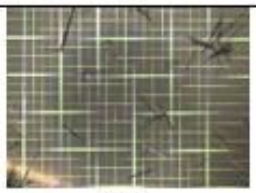 364 3.55	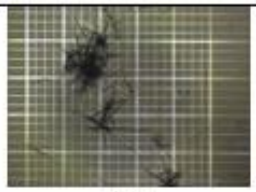 1040 3.76	 657 3.58
12.5ug/ml BSM	 170 0.82	 323 2.43	 453 3.55	 589 2.91
25ug/ml BSM	 179 1.34	 271 2.57	 410 2.65	 408 3.43
50ug/ml BSM	 97.3 1.97	 257 2.05	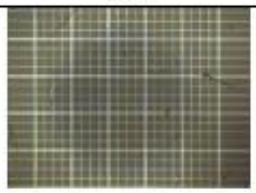 186 5.30	 246 5.93
The top row of data is the average crystal quantity and the bottom row is the average longest crystal length per the specific test group and time.				

	Time (hr)			
Concentration	24	48	72	96
0ug/ml (PBS)			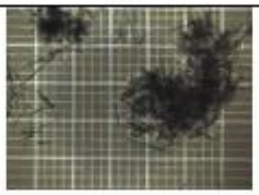	
	507 2.05	364 3.55	1040 3.76	657 3.58
12.5ug/ml rhPGR4			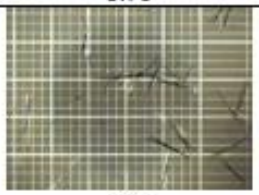	
	132 3.12	301 3.12	526 3.93	543 4.22
25ug/ml rhPRG4				
	3.00 0.00	28.7 1.26	93.0 2.57	111 2.96
50ug/ml rhPRG4				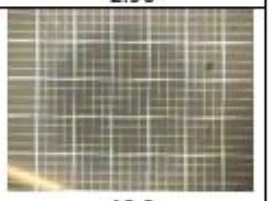
	1.66 0.00	9.00 0.00	14.0 1.50	13.3 1.33
The top row of data is the average crystal quantity and the bottom row is the average longest crystal length per the specific test group and time.				

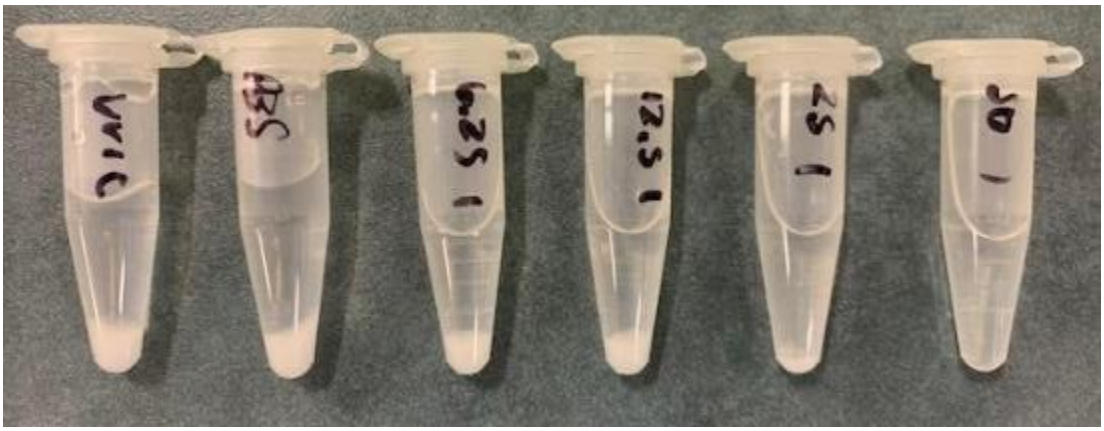

The figure 9 above shows t=96hr rhPRG4 test samples, including the Uric Acid (0mcg/ml), PBS (0mcg/ml), 6.25mcg/ml, 12.5mcg/ml, 25mcg/ml, and 50mcg/ml. The crystal can be clearly seen as the white material that collected at the bottom of the centrifuge tube, and the decrease of crystal material as the concentration of rhPRG4 increases is apparent. This mirrors the 10x magnified crystal images along with the length and quantity data.

Figure 10.

rhPRG4 inhibits MSU crystal formation from its saturated solution state, count

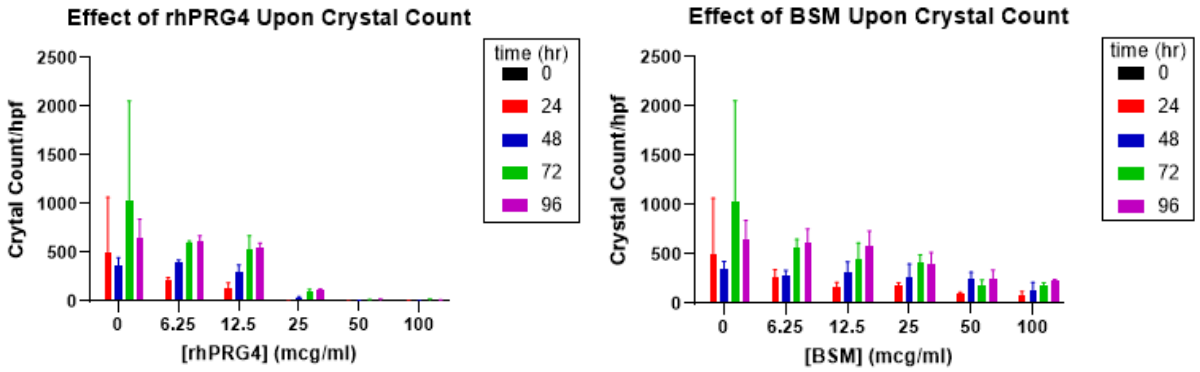

Legend: rhPRG4 or bovine submaxillary mucin (BSM) were added to a saturated solution of MSU at 37°C, then incubated at 35°C for 4 days. At 24 hour intervals, the number of MSU crystals formed were counted under magnification with a hemocytometer. Measurements were taken in triplicate and included crystal quantity and images. The crystal quantity measurements showed that as the rhPRG4 concentration increased, the number of crystals decreased but the BSM did not show a trend in concentration. Increased concentrations of rhPRG4 inhibited MSU crystal formation. The 0 mcg/ml concentration standard deviation is due to the high number of crystals clumping together and the difficultly due to measuring. Mean with standard deviation of crystal count per high power field is shown.

Data for crystal count was statistically evaluated via Anova, Tukey's multiple comparisons test across time and different concentrations. The statistically significant comparisons are shown below in the Table 2 & 3, and 4 & 5 for BSM and rhPRG4 respectively.

Table 2. BSM Crystal Count/hpf, Time					
Tukey's multiple comparisons test	Mean Diff.	95% CI of diff.	Below threshold?	Summary	Adjusted P Value
0 mcg/ml					
0 vs. 72 hours	-1040	-1561 to -519.3	Yes	****	<0.0001
0 vs. 96 hours	-657.3	-1178 to -136.3	Yes	**	0.0066
24 vs. 72 hours	-533.3	-1054 to -12.34	Yes	*	0.0423
48 vs. 72 hours	-696.7	-1218 to -175.7	Yes	**	0.0034
6.25 mcg/ml					
0 vs. 72 hours	-571.0	-1092 to -50.01	Yes	*	0.0248
0 vs. 96 hours	-619.7	-1141 to -98.67	Yes	*	0.0120
12.5 mcg/ml					
0 vs. 96 hours	-589.0	-1110 to -68.01	Yes	*	0.0191

Table 3. BSM Crystal Count/hpf, Concentration					
Tukey's multiple comparisons test	Mean Diff.	95% CI of diff.	Below threshold?	Summary	Adjusted P Value
72 hours					
0 vs. 12.5 mcg/ml	586.7	41.34 to 1132	Yes	*	0.0279
0 vs. 25 mcg/ml	630.0	84.68 to 1175	Yes	*	0.0145
0 vs. 50 mcg/ml	854.3	309.0 to 1400	Yes	***	0.0003
0 vs. 100 mcg/ml	850.0	304.7 to 1395	Yes	***	0.0003

Table 4. rhPRG4 Crystal Count/hpf, Time					
Tukey's multiple comparisons test	Mean Diff.	95% CI of diff.	Below threshold?	Summary	Adjusted P Value
0 mcg/ml					
0 vs. 24 hours	-507.0	-1008 to -5.768	Yes	*	0.0461
0 vs. 72 hours	-1040	-1542 to -539.1	Yes	****	<0.0001
0 vs. 96 hours	-657.3	-1159 to -156.1	Yes	**	0.0043
24 vs. 72 hours	-533.3	-1035 to -32.10	Yes	*	0.0316
48 vs. 72 hours	-678.7	-1180 to -177.4	Yes	**	0.0030
6.25 mcg/ml					
0 vs. 72 hours	-604.3	-1106 to -103.1	Yes	*	0.0105
0 vs. 96 hours	-615.7	-1117 to -114.4	Yes	**	0.0087
12.5 mcg/ml					
0 vs. 72 hours	-526.7	-1028 to -25.43	Yes	*	0.0348
0 vs. 96 hours	-543.3	-1045 to -42.10	Yes	*	0.0272

Table 5. rhPRG4 Crystal Count/hpf, Concentration					
Tukey's multiple comparisons test	Mean Diff.	95% CI of diff.	Below threshold?	Summary	Adjusted P Value
72 hours					
0 vs. 25 mcg/ml	947.3	422.7 to 1472	Yes	****	<0.0001
0 vs. 50 mcg/ml	1026	501.7 to 1551	Yes	****	<0.0001
0 vs. 100 mcg/ml	1027	502.0 to 1551	Yes	****	<0.0001
6.25 vs. 50 mcg/ml	590.3	65.69 to 1115	Yes	*	0.0187
6.25 vs. 100 mcg/ml	590.7	66.03 to 1115	Yes	*	0.0186
96 hours					
0 vs. 25 mcg/ml	545.7	21.03 to 1070	Yes	*	0.0369
0 vs. 50 mcg/ml	644.0	119.4 to 1169	Yes	**	0.0078

0 vs. 100 mcg/ml	649.3	124.7 to 1174	Yes	**	0.0071
6.25 vs. 50 mcg/ml	602.3	77.69 to 1127	Yes	*	0.0154
6.25 vs. 100 mcg/ml	607.7	83.03 to 1132	Yes	*	0.0142
12.5 vs. 50 mcg/ml	530.0	5.360 to 1055	Yes	*	0.0463
12.5 vs. 100 mcg/ml	535.3	10.69 to 1060	Yes	*	0.0429

Figure 11.

rhPRG4 inhibits MSU crystal formation from its saturated solution state, length

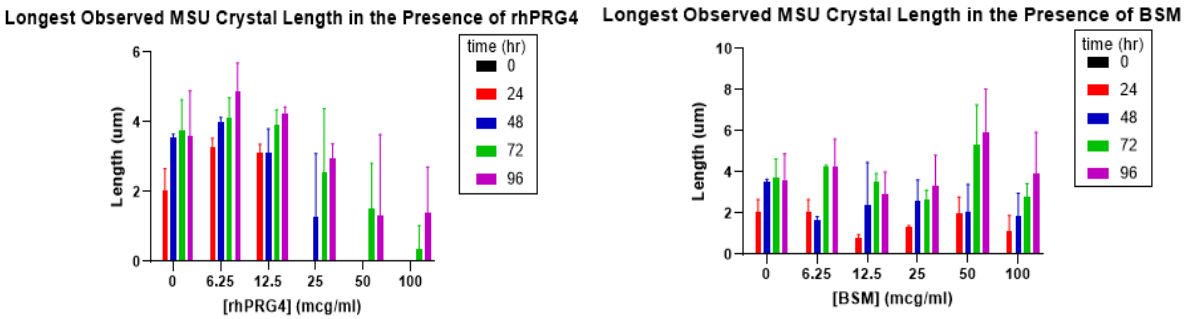

Legend: rhPRG4 or bovine submaxillary mucin (BSM) were added to a saturated state of MSU crystals at 37°C, then incubated at 35°C for 4 days. At 24 hour intervals, measurements were taken in triplicate and included images, and length of the longest crystal in center cell of the hemocytometer. The MSU crystal length increased at each 24 hour interval, and as the rhPRG4 concentration decreased. The MSU crystal length in BSM saturated solution did not show a trend per concentration but did show an increase in length at each time interval. Higher concentrations of rhPRG4 inhibited MSU size. Mean with standard deviation needle length is shown.

Data for needle length was statistically evaluated via Anova, Tukey's multiple comparisons test across time and different concentrations. The statistically significant comparisons are shown below in Tables 6 & 7, and 8 & 9 for BSM and rhPRG4 respectively.

Table 6. BSM Length (μm), Time					
Tukey's multiple comparisons test	Mean Diff.	95% CI of diff.	Below threshold?	Summary	Adjusted P Value
0 mcg/ml					
0 vs. 48 hours	-3.553	-5.900 to -1.206	Yes	***	0.0007
0 vs. 72 hours	-3.760	-6.107 to -1.413	Yes	***	0.0003
0 vs. 96 hours	-3.587	-5.934 to -1.240	Yes	***	0.0006
6.25 mcg/ml					
0 vs. 72 hours	-4.257	-6.604 to -1.910	Yes	****	<0.0001
0 vs. 96 hours	-4.240	-6.587 to -1.893	Yes	****	<0.0001
48 vs. 72 hours	-2.610	-4.957 to -0.2631	Yes	*	0.0220
48 vs. 96 hours	-2.593	-4.940 to -0.2464	Yes	*	0.0232
12.5 mcg/ml					
0 vs. 48 hours	-2.427	-4.774 to -0.07976	Yes	*	0.0393
0 vs. 72 hours	-3.557	-5.904 to -1.210	Yes	***	0.0007
0 vs. 96 hours	-2.913	-5.260 to -0.5664	Yes	**	0.0078
24 vs. 72 hours	-2.733	-5.080 to -0.3864	Yes	*	0.0146
25 mcg/ml					
0 vs. 48 hours	-2.573	-4.920 to -0.2264	Yes	*	0.0248
0 vs. 72 hours	-2.657	-5.004 to -0.3098	Yes	*	0.0188
0 vs. 96 hours	-3.317	-5.664 to -0.9698	Yes	**	0.0017
50 mcg/ml					
0 vs. 72 hours	-5.300	-7.647 to -2.953	Yes	****	<0.0001
0 vs. 96 hours	-5.933	-8.280 to -3.586	Yes	****	<0.0001

24 vs. 72 hours	-3.330	-5.677 to -0.9831	Yes	**	0.0017
24 vs. 96 hours	-3.963	-6.310 to -1.616	Yes	***	0.0001
48 vs. 72 hours	-3.243	-5.590 to -0.8964	Yes	**	0.0023
48 vs. 96 hours	-3.877	-6.224 to -1.530	Yes	***	0.0002
100 mcg/ml					
0 vs. 72 hours	-2.800	-5.147 to -0.4531	Yes	*	0.0116
0 vs. 96 hours	-3.957	-6.304 to -1.610	Yes	***	0.0001
24 vs. 96 hours	-2.817	-5.164 to -0.4698	Yes	*	0.0110

Table 7. BSM Length (μm), Concentration					
Tukey's multiple comparisons test	Mean Diff.	95% CI of diff.	Below threshold?	Summary	Adjusted P Value
96 hours					
12.5 vs. 50 mcg/ml	-3.020	-5.477 to -0.5635	Yes	**	0.0077
25 vs. 50 mcg/ml	-2.617	-5.073 to -0.1602	Yes	*	0.0303

Table 8. rhPRG4 Length (μm), Time					
Tukey's multiple comparisons test	Mean Diff.	95% CI of diff.	Below threshold?	Summary	Adjusted P Value
0 mcg/ml					
0 vs. 24 hours	-2.057	-3.964 to -0.1491	Yes	*	0.0284
0 vs. 48 hours	-3.553	-5.461 to -1.646	Yes	****	<0.0001
0 vs. 72 hours	-3.760	-5.668 to -1.852	Yes	****	<0.0001
0 vs. 96 hours	-3.587	-5.494 to -1.679	Yes	****	<0.0001
6.25 mcg/ml					
0 vs. 24 hours	-3.290	-5.198 to -1.382	Yes	****	<0.0001
0 vs. 48 hours	-3.993	-5.901 to -2.086	Yes	****	<0.0001
0 vs. 72 hours	-4.100	-6.008 to -2.192	Yes	****	<0.0001

0 vs. 96 hours	-4.893	-6.801 to -2.986	Yes	****	<0.0001
12.5 mcg/ml					
0 vs. 24 hours	-3.127	-5.034 to -1.219	Yes	***	0.0002
0 vs. 48 hours	-3.127	-5.034 to -1.219	Yes	***	0.0002
0 vs. 72 hours	-3.930	-5.838 to -2.022	Yes	****	<0.0001
0 vs. 96 hours	-4.223	-6.131 to -2.316	Yes	****	<0.0001
25 mcg/ml					
0 vs. 72 hours	-2.573	-4.481 to -0.6658	Yes	**	0.0031
0 vs. 96 hours	-2.963	-4.871 to -1.056	Yes	***	0.0005
24 vs. 72 hours	-2.573	-4.481 to -0.6658	Yes	**	0.0031
24 vs. 96 hours	-2.963	-4.871 to -1.056	Yes	***	0.0005

Table 9. rhPRG4 Length (μm), Concentration

Tukey's multiple comparisons test	Mean Diff.	95% CI of diff.	Below threshold?	Summary	Adjusted P Value
24 hours					
0 vs. 25 mcg/ml	2.057	0.06007 to 4.053	Yes	*	0.0399
0 vs. 50 mcg/ml	2.057	0.06007 to 4.053	Yes	*	0.0399
0 vs. 100 mcg/ml	2.057	0.06007 to 4.053	Yes	*	0.0399
6.25 vs. 25 mcg/ml	3.290	1.293 to 5.287	Yes	***	0.0001
6.25 vs. 50 mcg/ml	3.290	1.293 to 5.287	Yes	***	0.0001
6.25 vs. 100 mcg/ml	3.290	1.293 to 5.287	Yes	***	0.0001
12.5 vs. 25 mcg/ml	3.127	1.130 to 5.123	Yes	***	0.0003
12.5 vs. 50 mcg/ml	3.127	1.130 to 5.123	Yes	***	0.0003
12.5 vs. 100 mcg/ml	3.127	1.130 to 5.123	Yes	***	0.0003
48 hours					
0 vs. 25 mcg/ml	2.293	0.2967 to 4.290	Yes	*	0.0154
0 vs. 50 mcg/ml	3.553	1.557 to 5.550	Yes	****	<0.0001

0 vs. 100 mcg/ml	3.553	1.557 to 5.550	Yes	****	<0.0001
6.25 vs. 25 mcg/ml	2.733	0.7367 to 4.730	Yes	**	0.0021
6.25 vs. 50 mcg/ml	3.993	1.997 to 5.990	Yes	****	<0.0001
6.25 vs. 100 mcg/ml	3.993	1.997 to 5.990	Yes	****	<0.0001
12.5 vs. 50 mcg/ml	3.127	1.130 to 5.123	Yes	***	0.0003
12.5 vs. 100 mcg/ml	3.127	1.130 to 5.123	Yes	***	0.0003
72 hours					
0 vs. 50 mcg/ml	2.257	0.2601 to 4.253	Yes	*	0.0179
0 vs. 100 mcg/ml	3.380	1.383 to 5.377	Yes	****	<0.0001
6.25 vs. 50 mcg/ml	2.597	0.6001 to 4.593	Yes	**	0.0040
6.25 vs. 100 mcg/ml	3.720	1.723 to 5.717	Yes	****	<0.0001
12.5 vs. 50 mcg/ml	2.427	0.4301 to 4.423	Yes	**	0.0087
12.5 vs. 100 mcg/ml	3.550	1.553 to 5.547	Yes	****	<0.0001
25 vs. 100 mcg/ml	2.193	0.1967 to 4.190	Yes	*	0.0232
96 hours					
0 vs. 50 mcg/ml	2.253	0.2567 to 4.250	Yes	*	0.0182
0 vs. 100 mcg/ml	2.170	0.1734 to 4.167	Yes	*	0.0255
6.25 vs. 50 mcg/ml	3.560	1.563 to 5.557	Yes	****	<0.0001
6.25 vs. 100 mcg/ml	3.477	1.480 to 5.473	Yes	****	<0.0001
12.5 vs. 50 mcg/ml	2.890	0.8934 to 4.887	Yes	***	0.0010
12.5 vs. 100 mcg/ml	2.807	0.8101 to 4.803	Yes	**	0.0015

MSU & *Prg4*$^{-/-}$ Cell Macrophage ELISA Testing in the Absence and Presence of rhPRG4

Figure 12.

PRG4 biofouled MSU crystals reduces IL1 and CXCL levels in Prg4$^{-/-}$ *macrophages*

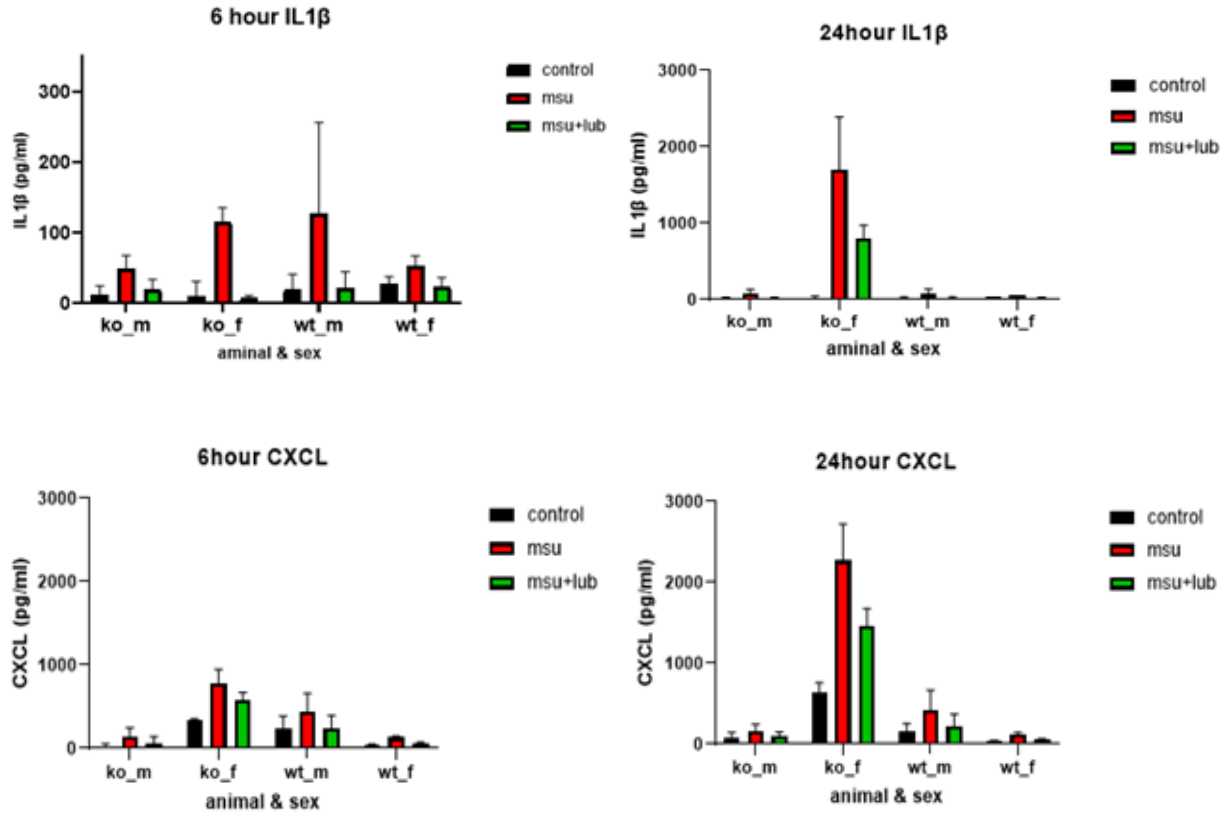

Legend: Secreted IL1β and CXCL levels for *Prg4*$^{-/-}$ peritoneal macrophages exposed to MSU crystals biofouled with rhPRG4.

Pyrogen free MSU crystals, as described in the methods, were exposed to rhRG4 and washed extensively, then introduced to *Prg4*$^{-/-}$ peritoneal macrophages and showed significantly lower secretion of IL1β (Table 10) after 6 hrs of incubation. No crystals were introduced in the control group, non-biofouled MSU crystals were introduced in the MSU group, and rhPRG4 biofouled MSU crystals were introduced in the MSU+L group. Analysis at 6 hours (Table 10 & 12) showed significantly higher levels of IL1β which was even more so observed at 24 hours (Table 11 & 13) in the MSU groups. *Prg4* null (*Prg4*$^{-/-}$) (ko_f,

ko_m) and Wild type (*Prg4*$^{+/+}$) (wt_f, wt_m) animals of both sexes were tested where sex and Prg4 status were dependent variables. Female *Prg4*$^{-/-}$ animals expressed higher IL1β and CXCL levels in all studies. All data is shown as mean values with standard deviation.

The 6 hour and 24 hour IL1β data was statistically evaluated via Anova, Tukey's multiple comparisons test looking at control vs MSU vs MSU+L (Table 10 & 11) and *Prg4*$^{-/-}$ female vs *Prg4*$^{-/-}$ male vs wildtype female vs wildtype male (ko_f vs Ko_m vs wt_m vs wt_f) (Table 12 & 13). The statistically significant findings are shown in the table below.

Table 10. 6 hour IL1β test group

Tukey's multiple comparisons test	Predicted (LS) mean diff.	95% CI of diff.	Below threshold?	Summary	Adjusted P Value
ko_m					
control vs. msu	-38.22	-75.36 to -1.081	Yes	*	0.0421
ko_f					
control vs. msu	-105.6	-158.4 to -52.70	Yes	****	<0.0001
msu vs. msu+L	108.1	52.41 to 163.8	Yes	****	<0.0001
wt_m					
control vs. msu	-107.7	-144.8 to -70.53	Yes	****	<0.0001
msu vs. msu+L	105.0	67.86 to 142.1	Yes	****	<0.0001

Table 11. 24 hour IL1β test group

Tukey's multiple comparisons test	Predicted (LS) mean diff.	95% CI of diff.	Below threshold?	Summary	Adjusted P Value
ko_f					
control vs. msu	-1671	-1876 to -1465	Yes	****	<0.0001
control vs. msu+L	-779.1	-984.4 to -573.7	Yes	****	<0.0001
msu vs. msu+L	891.5	701.4 to 1082	Yes	****	<0.0001

Table 12. 6 hour IL1β animal group					
Tukey's multiple comparisons test	Predicted (LS) mean diff.	95% CI of diff.	Below threshold?	Summary	Adjusted P Value
msu					
ko_m vs. ko_f	-65.69	-117.7 to -13.73	Yes	**	0.0069
ko_m vs. wt_m	-76.50	-117.3 to -35.74	Yes	****	<0.0001
wt_m vs. wt_f	72.67	22.74 to 122.6	Yes	**	0.0013

Table 13. 24 hour IL1β animal group					
Tukey's multiple comparisons test	Predicted (LS) mean diff.	95% CI of diff.	Below threshold?	Summary	Adjusted P Value
msu					
ko_m vs. ko_f	-1607	-1784 to -1429	Yes	****	<0.0001
ko_f vs. wt_m	1623	1446 to 1800	Yes	****	<0.0001
ko_f vs. wt_f	1645	1442 to 1848	Yes	****	<0.0001
msu+L					
ko_m vs. ko_f	-783.7	-961.0 to -606.4	Yes	****	<0.0001
ko_f vs. wt_m	785.4	608.1 to 962.7	Yes	****	<0.0001
ko_f vs. wt_f	780.1	577.4 to 982.9	Yes	****	<0.0001

Analysis at 6 hours (Table 14 & 16) showed significantly higher levels of CXCL which was even more so observed at 24hours (Table 15 & 17) in each MSU group. *Prg4* null (*Prg4*$^{-/-}$) (ko_f, ko_m) and Wild type (*Prg4*$^{+/+}$) (wt_f, wt_m) animals of both sexes were tested where sex and Prg4 status were dependent variables. Female *Prg4*$^{-/-}$ animals expressed higher IL1β and CXCL levels in all studies. All data is shown as mean values with standard deviation.

The 6 hour and 24 hour CXCL data was statistically evaluated via Anova, Tukey's multiple comparisons test looking at control vs MSU vs MSU+L (Table 14 & 15) and *Prg4*$^{-/-}$ female vs *Prg4*$^{-/-}$ male vs wildtype

female vs wildtype male (ko_f vs Ko_m vs wt_m vs wt_f) (Table 16 & 17). The statistically significant findings are shown in the table below

Table 14. 6 hour CXCL test group					
Tukey's multiple comparisons test	Predicted (LS) mean diff.	95% CI of diff.	Below threshold?	Summary	Adjusted P Value
ko_f					
control vs. msu	-449.7	-677.5 to -221.9	Yes	****	<0.0001
control vs. msu+L	-243.7	-471.5 to -15.86	Yes	*	0.0331
wt_m					
control vs. msu	-205.7	-319.6 to -91.77	Yes	***	0.0001
msu vs. msu+L	197.9	81.39 to 314.3	Yes	***	0.0003

Table 15. 24 hour CXCL test group					
Tukey's multiple comparisons test	Predicted (LS) mean diff.	95% CI of diff.	Below threshold?	Summary	Adjusted P Value
ko_f					
control vs. msu	-1625	-1881 to -1370	Yes	****	<0.0001
control vs. msu+L	-817.7	-1073 to -562.0	Yes	****	<0.0001
msu vs. msu+L	807.7	552.0 to 1063	Yes	****	<0.0001
wt_m					
control vs. msu	-273.9	-407.4 to -140.4	Yes	****	<0.0001
msu vs. msu+L	202.0	68.50 to 335.5	Yes	**	0.0015
wt_f					
control vs. msu	-89.00	-236.6 to 58.59	No	ns	0.3266
control vs. msu+L	-13.67	-161.3 to 133.9	No	ns	0.9735
msu vs. msu+L	75.33	-72.26 to 222.9	No	ns	0.4469

Table 16. 6hour CXCL animal group					
Tukey's multiple comparisons test	Predicted (LS) mean diff.	95% CI of diff.	Below threshold?	Summary	Adjusted P Value
control					
ko_m vs. ko_f	-309.9	-507.7 to -112.1	Yes	***	0.0005
ko_m vs. wt_m	-207.8	-332.9 to -82.73	Yes	***	0.0002
ko_f vs. wt_f	299.1	94.82 to 503.4	Yes	**	0.0013
wt_m vs. wt_f	197.0	61.90 to 332.2	Yes	**	0.0014
msu					
ko_m vs. ko_f	-646.6	-844.4 to -448.8	Yes	****	<0.0001
ko_m vs. wt_m	-300.5	-425.6 to -175.4	Yes	****	<0.0001
ko_f vs. wt_m	346.1	148.3 to 543.9	Yes	****	<0.0001
ko_f vs. wt_f	657.4	453.2 to 861.7	Yes	****	<0.0001
wt_m vs. wt_f	311.4	176.2 to 446.5	Yes	****	<0.0001
msu+L					
ko_m vs. ko_f	-517.8	-715.6 to -320.0	Yes	****	<0.0001
ko_m vs. wt_m	-179.9	-307.8 to -51.98	Yes	**	0.0022
ko_f vs. wt_m	337.9	138.3 to 537.5	Yes	***	0.0001
ko_f vs. wt_f	522.2	317.9 to 726.5	Yes	****	<0.0001
wt_m vs. wt_f	184.3	46.55 to 322.0	Yes	**	0.0039

Table 17. 24 hour CXCL animal group					
Tukey's multiple comparisons test	Predicted (LS) mean diff.	95% CI of diff.	Below threshold?	Summary	Adjusted P Value
control					
ko_m vs. ko_f	-575.4	-797.4 to -353.4	Yes	****	<0.0001
ko_f vs. wt_m	493.8	269.9 to 717.8	Yes	****	<0.0001
ko_f vs. wt_f	607.0	377.7 to 836.3	Yes	****	<0.0001

msu					
ko_m vs. ko_f	-2109	-2331 to -1887	Yes	****	<0.0001
ko_m vs. wt_m	-264.0	-407.5 to -120.4	Yes	****	<0.0001
ko_f vs. wt_m	1845	1621 to 2069	Yes	****	<0.0001
ko_f vs. wt_f	2143	1914 to 2373	Yes	****	<0.0001
wt_m vs. wt_f	298.1	143.5 to 452.6	Yes	****	<0.0001
msu+L					
ko_m vs. ko_f	-1369	-1590 to -1147	Yes	****	<0.0001
ko_f vs. wt_m	1240	1016 to 1464	Yes	****	<0.0001
ko_f vs. wt_f	1411	1182 to 1640	Yes	****	<0.0001
wt_m vs. wt_f	171.4	16.83 to 326.0	Yes	*	0.0236

In vivo DigiGait Mouse Analysis - IA injected *Prg4* conditional mice with MSU crystal

The conditional *Prg4* mouse model used expresses Prg4 naturally but that expression is silenced by Cre activation upon the IP injection of tamoxifen. All DigiGait metrics were captured, the selected metrics are detailed below including graphical and statistically significant analysis (Lakes, 2016). These metrics were selected due to the potential relevance to the study outcomes and includes data for swing time, stance time, stride length, and belt speed data. All metric data have been prepared for future statistical analysis. The methods and techniques used in this study were informed by an earlier effort using HDV-EF1-*Prg4* IA injected *Prg4*$^{-/-}$ mice which was an attempt to convert the *Prg4* null mouse into a Prg4 expressing animal. Data from that effort has been included in the Appendix.

Figure 13.

MSU crystal PRG4 conditional mice gait analysis

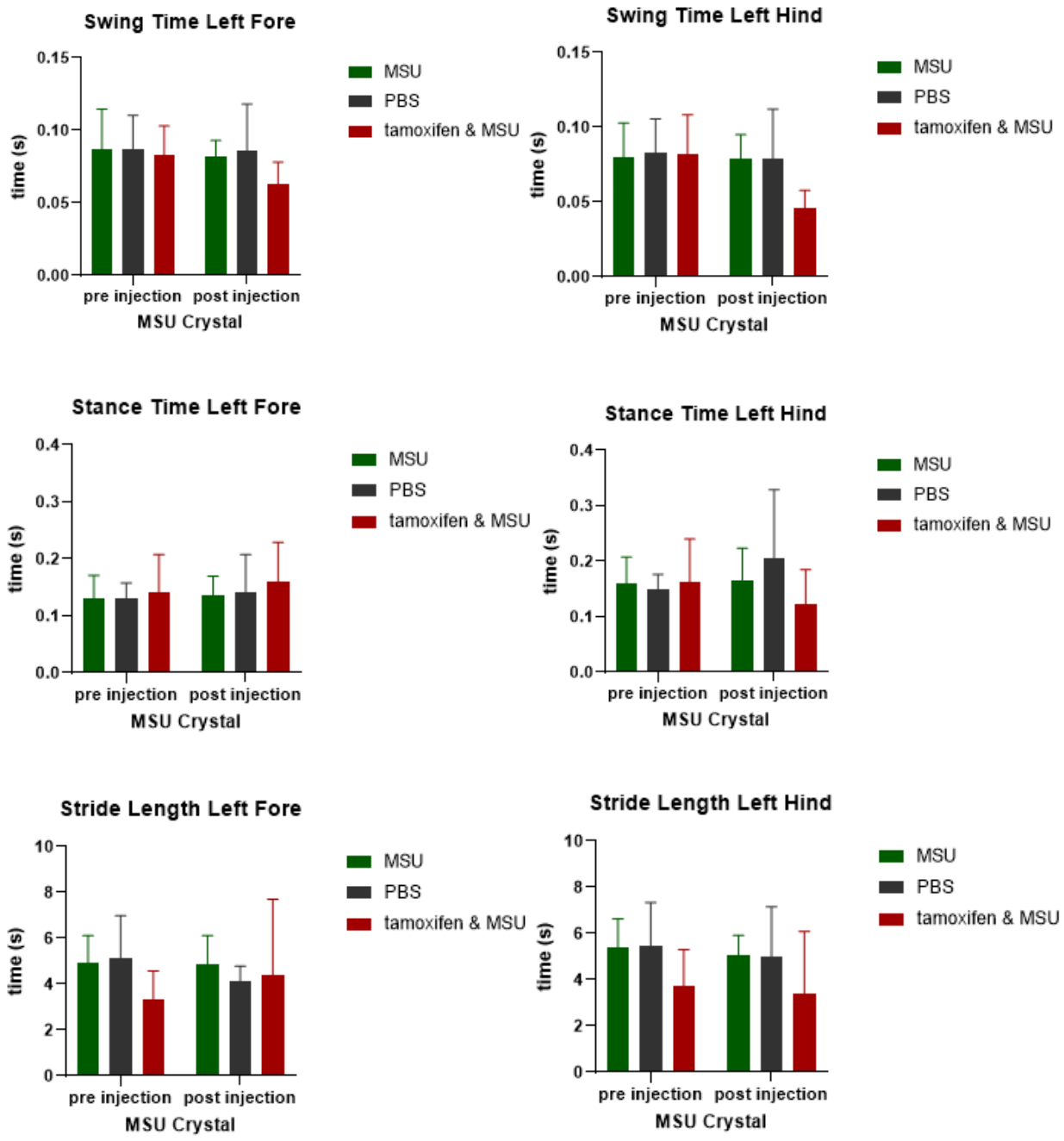

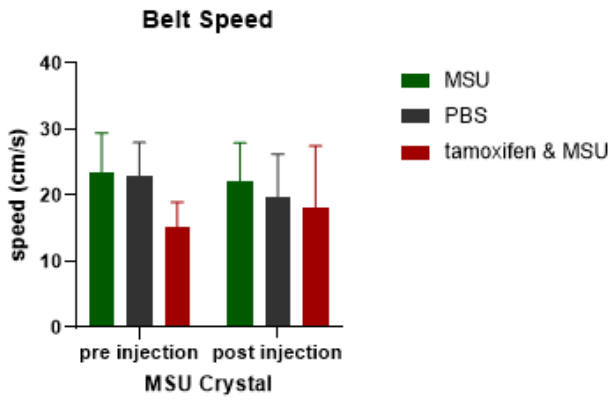

Legend: Prg4 expressing animals that had not received tamoxifen maintained consistent gait measurements, similar to controls, versus the non-Prg4 expressing animals when receiving MSU crystal injections.

Prg4 conditional knockout mice received tamoxifen IP injections 8 weeks prior to MSU crystal IA injections in both hind limbs then underwent DigiGait analysis. All animals were *Prg4* mouse mutants, the MSU group did not receive the tamoxifen injections therefore were producing Prg4 and did receive the MSU injections. The tamoxifen & MSU group did receive both the tamoxifen and MSU crystal injection. The PBS group received PBS in place of tamoxifen and did not receive the MSU crystal injection.

There were differences in gait performance for all metrics between the MSU and tamoxifen & MSU group. Swing time, stride length, and belt speed were all greater pre- and post-injection in the MSU vs MSU & tamoxifen group. Specifically between pre- and post-injection metrics, swing time (left hind) in the MSU & tamoxifen group had the largest difference of average pre-injection 0.082s vs average post-injection 0.046s. There is greater expected difference between groups in the hind limbs compared to fore limbs because the MSU injection was in the hind limbs. Stride length was also decreased between the MSU & tamoxifen and MSU group, which is a marker of arthrosis models (Table 19). This data suggests that there is a difference in gait for the animal groups injected with MSU crystals when they do and do not

produce Prg4 (typically lower values when not producing Prg4). The belt speed for testing also shows a difference between the tamoxifen & MSU (average 15.2cm/s pre-injection) and other groups (average 23.5cm/s MSU pre-injection), which is reflective of the animal reluctance to walk.

Table 18. Swing Time, Left Hind					
Tukey's multiple comparisons test	Predicted (LS) mean diff.	95% CI of diff.	Below threshold?	Summary	Adjusted P Value
post injection					
MSU vs. tamoxifen & MSU	0.03321	0.003856 to 0.06257	Yes	*	0.0245

Table 19. MOUSE SPECIFICS, INC. DigiGaitTM Imaging System – Selected Indices			
Index Metric	Units	Definition	Example, Application, or Reference
Swing Time	s	Time duration of the swing phase (no paw contact with belt)	Swing duration decreases with increasing speed, and there is a limit on how brief swing duration can be. Arthritic animals may have increased swing duration because of loss of mobility of the joints. Swing duration increases with pain (Vrinten and Hamers, *Pain* 102:203-209, 2003). Longer swing in the forelimbs might provide mice with ample opportunity for limb placement prior to weight bearing (Clarke and Still, *Behav Res Methods*, 33:422-426, 2001, Budsberg et al. *Am J Vet Res* 48:915-918, 1987).
Stance Time	s	Time duration of the stance duration (paw contact with belt). Stance duration is equal to the sum of braking duration and propulsion duration).	Stance duration will decrease with increased speed. Moreover, with increased speed, stance duration will decrease to a greater extent than swing duration.
Stride Length	cm	The spatial length that a paw traverses through a given stride.	Distance between successive strides of the same paw. This number should normally be nearly equivalent among the 4 paws of a given animal (Hannigan and Riley, *Alcohol*, 5:451- 454, 1989). Prenatal and neonatal ethanol exposure results in significantly shorter stride length. As rodents increase walking speed, stride length increases and stance duration decreases (Hruska RE et al. *Life Sciences* 25:171-180, 1979). Mice with arthritis also have shorter stride length (Williams et al., *J Bone Joint Surg* 11:172-180, 1993).

Chapter 4: Discussion and Conclusions

Lubricin & MSU Crystal Interaction

The primary focus of this thesis was to understand the interaction between rhPRG4 and concentrated MSU in solution and MSU crystals relating to gout: using both *in vitro, ex vivo,* and *in vivo* methods. There are obvious and clear significant differences between test groups for these data sets. The results indicate that there are other PRG4-dependent mechanisms which could mitigate both acute and chronic gout. As mentioned above, gout is increasingly prevalent with limited number of treatment methods, particularly in its acute manifestations. Gout attacks recur, and thus present elevated costs that can range from $172-$6179 (Rai, 2015), typical of a frequently reoccurring disease. Thus other preventative treatments would provide value to patients' and health care systems at large.

The initial test of MSU crystal growth and length with rhPRG4 and BSM showed that rhPRG4 inhibits MSU crystal formation from its saturated solution state. This was apparent in both crystal quantity and length over time, as compared to BSM as control (Fig. 9-11). BSM was selected as a control due to the similarity in mucin structure, to begin to investigate if and why rhPRG4 might inhibit MSU crystal formation. The limitation of this study was the use of borate buffer which is needed to render MSU into solution, but is non physiologic, thus we can only presume the same effect we are seeing *in vitro* is also occurring *in vivo*. In AFGP the hydrophobic aspect of the Ala-Ala-Thr is thought to interact with the sheets of crystallizing water which then orients the Thr-O linked glycosylation away which disrupts water (Furukawa, 2019). Assuming the sugars may be causing the disruption, in both instances the protein backbone is interacting with a surface.

This study was followed by assessing the IL-1β and CXCL macrophage expression via ELISA from *Prg4*$^{-/-}$ mouse macrophages exposed to pre-formed MSU crystals that had been biofouled with rhPRG4 (Fig. 12). IL-1β and CXCL were selected because both are released by macrophages when MSU crystals

are present. This informs us that the cells have NLRP3 activation and the CXCL indicates there is neutrophil recruitment and neutrophilic inflammation taking place (Busso, 2010). The results of this study showed that for ELISA measured expression for IL-1β and CXCL, there were statistically significant differences between 6 and 24 hours, between the sexes, and between some of the test groups. This indicates that the rhPRG4 on the crystals blunted the inflammatory response which would otherwise ensue. These *ex vivo* results also tell us that what we observed *in vitro* above does likely have some role (despite the borate buffer) since rhPRG4 is indeed interacting with MSU on its surface- in much the same way it interfered with nucleation and how AFGP interacts with solid water to prevent growth via crystallization. A limitation to this study is that we did not directly observe rhPRG4 on the crystal surfaces. This could have been conducted via an antibody probing approach.

As time increased, the expressed levels of IL-1β and CXCL increased, as was expected. The animal groups were separated by gender to determine if there were any sex based differences. These became more apparent in the 24 hour time study. Particularly for the *Prg4*$^{-/-}$ mice group there was a significant difference in expression between male and female mice, with female mice expressing more IL-1β and CXCL levels. These observations based on difference in sex are supported by other works, including the findings of a urate oxidase (Uox-knockout) mouse model where male and female mice developed differing hyperuricemia induced disorders (Lu, 2018). The difference in inflammatory marker expression between sexes warrants future investigation as there is a discrepancy between prevalence in gout based on sex as it is more common in men (Singh, 2013). Most importantly, within each animal group and time, the MSU crystals incubated with rhPRG4 suppressed the IL-1β and CXCL compared to the MSU crystal test group (Fig. 12).

It is clear from these data that rhPRG4 is inhibiting MSU crystal formation and MSU phagocytosis, but the precise mechanism of action is currently unknown. Future research and ongoing efforts are being

conducted to model the lubricin molecule. This will be used to determine the interactions between MSU crystals & lubricin.

Lastly, it was clear in the DigiGait mouse analysis - MSU crystal injected *Prg4*$^{-/-}$ mice data that there were gait differences between the *Prg4*$^{-/-}$ mice that did and did not receive tamoxifen injections as these were not or were expressing Prg4 respectively (Fig. 14). It is also promising that there was similar belt speed for the PBS and no tamoxifen group, showing similarity in gait speed, while the tamoxifen group animals were reluctant to walk and had observably lower belt speed. This data indicates that *Prg4* deficient mice that received MSU injections were more lame than the littermates that did not receive tamoxifen, and thus were still expressing *Prg4* which counteracted the MSU IA injection. The former group was only able to tolerate a lower belt speed. Arthritic animals may have increased swing duration because of loss of mobility of the joints. Swing duration increases with pain (Vrinten and Hamers, Pain 102:203-209, 2003). Longer swing in the forelimbs may provide mice with ample opportunity for limb placement prior to weight bearing.

The DigiGait system was used because while there are other existing methodologies to assess for disturbance in locomotion, most focus on disturbance in one limb only. To improve the measurable effect of this work, both hind limbs were affected so a quadruped gait system was needed. DigiGait does measure animal symmetry and it is useful for other arthritic models, but the additional metrics capable were suitable for study with multiple joints affected (Lakes, 2016). Prior studies have used DigiGait for symptomatic relief in a murine model of osteoarthritis (Plaas, 2011).

A limitation of the in vivo experiment is that Prg4$^{CreERt2/+}$ animals that had received tamoxifen (MSU & tamoxifen) and were no longer expressing Prg4 develop clinical CACP in that there is joint arthrosis which is still being characterized. As this is a well somewhat tolerated disorder in humans, work by the Jay lab has not identified a consistent gait disorder in these animals. It was only after these recombined

animals received IA MSU that the animals became lame. Histology is not available at the time of this writing to determine if an aggressive synovitis is present in the MSU IA injected group to complement the change in gait observed.

Current work using molecular dynamic simulations, specifically CHARMM carbohydrate force field, to study the structure, dynamics, and thermodynamics of lubricin glycoprotein was inspired by these results. trRosetta is being used to predict the mucin domain structures of lubricin. This work is being conducted by Brenda Rubenstein, Department of Chemistry, Brown University. This understanding would provide a potential mechanism of action for the downregulation of MSU crystal growth via lubricin (PRG4).

PRG4 concentrations in synovial fluid are maintained by the synovial membrane of 60kDa. The PRG4 concentration within synovial fluid is 180 mcg/ml nominally, but in serum is 0.5 mcg/ml. This discrepancy suggests PRG4 plays a fundamental role in joint homeostasis as it relates to tissue lubrication and metabolic homeostasis (Alquraini, 2015). The anti-inflammatory activity of PRG4 has already been described and reported (Reginato, 2016) (Qadri,2018). rhPRG4 was shown both in vitro and in vivo to be therapeutic in acute gout preclinical models (Qadri,2018).

The almost 400-fold difference in synovial vs serum concentration of PRG4 suggests that another PRG4-dependent mechanism to enable normal joint function are at work. The present work indicates that Prg4 not only presents an anti-inflammatory effect in acute gout but also abates the deleterious effects of hyperuricemia which otherwise results in crystal deposition and also prevents inflammation triggered by existing MSU crystals. This is a newly discovered attribute of PRG4 possibly unique to humans since other mammals in the animal kingdom do not develop gout. The phenomenon of MSU crystal inhibition appears to recapitulate the ice crystal nucleation inhibition by AFGP which allows a significant number of different fish species to survive in freezing temperatures.

Conclusion: As it relates to gout, PRG4 presents a redundant metabolic strategy to prevent gout. As shown in the present work it blocks nucleation of MSU crystals and phagocytosis of biofouled MSU crystals thus blunting acute inflammation in engulfing macrophages presented with PRG4-laden MSU crystal (Fig 14). This is graphically depicted by steps 2 and 3 in Fig. 14. Crystallization of compounds from aqueous solution can be disturbed by O-linked glycosylations and as observed is relevant to human disease. These post translational modifications are common in mucins which in turn occupy biological surfaces and play a prominent barrier role. Other diseases that are crystal dependent including oxalic acid and calcium pyrophosphate, are respectively relevant to renal stones and myositis, which may also be therapeutic targets for rhPRG4. Unanswered and important questions arising from this investigation include investigating the relationship between Camptodactyly-Arthropathy-Coxa vara-Pericarditis (CACP) syndrome and gout. Patients with CACP have no PRG4 secretion (Ciullini, 2014). It is unknown what the incidence and severity of gout is among patients with CACP as there is currently no disease registry but one is planned via the CACP Patient Foundation (CACP Research Foundation, n.d.).

Figure 14.

Gout Inflammation Pathway & rhPRG4 (Busso, 2010)

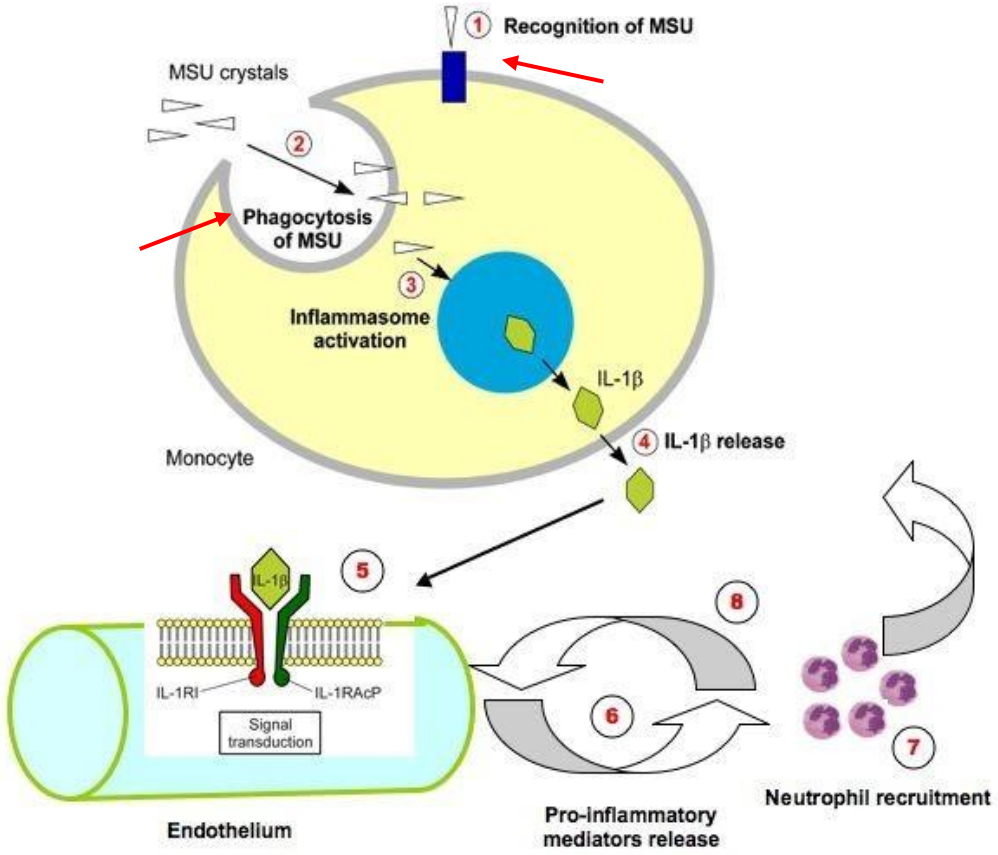

Legend: This figure details the cellular inflammatory pathway for gout. The present work has shown that MSU crystal nucleation and growth (step 2) is suppressed by rhPRG4. The inflammatory response of pre-existing MSU crystal may also be suppressed by rhPRG4 biofouling the crystal surface (step 2). The MSU crystal interaction with TLR receptors (step 1) in prior work was also shown to be inhibited by PRG4, was its inhibitory effects on NLRP3 activation (step 3) which is the absence of PRG4 results in cleavage of pro-IL-1β (step 4). Exposed endothelium nearly is also activated releasing chemokines like CXCL, IL-8, for neutrophil recruitment and additional proinflammatory compounds such as IL1β (step 5-8) (Busso, 2010).

References

Works Cited

Alquraini, A., Garguilo, S., D'Souza, G., Zhang, L. X., Schmidt, T. A., Jay, G. D., & Elsaid, K. A. (2015). The interaction of lubricin/proteoglycan 4 (PRG4) with toll-like receptors 2 and 4: an anti-inflammatory role of PRG4 in synovial fluid. *Arthritis research & therapy*, *17*, 353. https://doi.org/10.1186/s13075-015-0877-x

Busso, N., & So, A. (2010). Mechanisms of inflammation in gout. *Arthritis research & therapy*, *12*(2), 206. https://doi.org/10.1186/ar2952

CACP Research Foundation. (n.d.). *CACP Syndrome.* https://www.cacpresearchfoundation.org/cacp-syndrome-1

Choi, B. R., Lim, Y. H., Joo, K. B., Paik, S. S., Kim, N. S., Lee, J. K., & Yoo, D. H. (2004). Camptodactyly, arthropathy, coxa vara, pericarditis (CACP)syndrome: a case report. *Journal of Korean medical science*, *19*(6), 907–910. https://doi.org/10.3346/jkms.2004.19.6.907

Ciullini Mannurita, S., Vignoli, M., Bianchi, L., Kondi, A., Gerloni, V., Breda, L., Ten Cate, R., Alessio, M., Ravelli, A., Falcini, F., & Gambineri, E. (2014). CACP syndrome: identification of five novel mutations and of the first case of UPD in the largest European cohort. *European journal of human genetics: EJHG*, *22*(2), 197–201. https://doi.org/10.1038/ejhg.2013.123

Dalal, D. S., Mbuyi, N., Shah, I., Reinert, S., Hilliard, R., & Reginato, A. (2020). Prescription Opioid Use Among Patients With Acute Gout Discharged From the Emergency Department. *Arthritis Care & Research, 72*(8), 1163-1168. doi:10.1002/acr.23928

Dehlin, M., Jacobsson, L., & Roddy, E. (2020). Global epidemiology of gout: prevalence, incidence, treatment patterns and risk factors. *Nature reviews. Rheumatology*, *16*(7), 380–390. https://doi.org/10.1038/s41584-020-0441-1

Elsaid, K. A., Machan, J. T., Waller, K., Fleming, B. C., & Jay, G. D. (2009). The impact of anterior cruciate ligament injury on lubricin metabolism and the effect of inhibiting tumor necrosis factor alpha on

chondroprotection in an animal model. *Arthritis and rheumatism*, *60*(10), 2997–3006. https://doi.org/10.1002/art.24800

Emad, Y., Ragab, Y., Khalifa, M., Bassyouni, I., El-Shaarawy, N., & Rasker, J. J. (2013). Axial involvement with facet joint arthropathy and bony ankylosis in a case of camptodactyly, arthropathy, coxa vara, pericarditis (CACP) syndrome. *Joint bone spine*, *80*(5), 520–522. https://doi.org/10.1016/j.jbspin.2013.01.010

Engel, B., Just, J., Bleckwenn, M., & Weckbecker, K. (2017). Treatment Options for Gout. *Deutsches Aerzteblatt Online*. doi:10.3238/arztebl.2017.0215

Furukawa, Y., Nagashima, K., Nakatsubo, S., Zepeda, S., Murata, K. I., & Sazaki, G. (2019). Crystal-plane-dependent effects of antifreeze glycoprotein impurity for ice growth dynamics. *Philosophical transactions. Series A, Mathematical, physical, and engineering sciences*, *377*(2146), 20180393. https://doi.org/10.1098/rsta.2018.0393

Giubertoni, G., Meister, K., Devries, A. L., & Bakker, H. J. (2019). Determination of the Solution Structure of Antifreeze Glycoproteins Using Two-Dimensional Infrared Spectroscopy. *The Journal of Physical Chemistry Letters, 10*(3), 352-357. doi:10.1021/acs.jpclett.8b03468

Grassi, W., & De Angelis, R. (2012). Clinical features of gout. *Reumatismo*, *63*(4), 238–245. https://doi.org/10.4081/reumatismo.2011.238

Harding, M. M., Anderberg, P. I., & Haymet, A. D. (2003). Antifreeze glycoproteins from polar fish. *European Journal of Biochemistry, 270*(7), 1381-1392. doi:10.1046/j.1432-1033.2003.03488.x

Hosomi, A., Nakanishi, T., Fujita, T., & Tamai, I. (2012). Extra-Renal Elimination of Uric Acid via Intestinal Efflux Transporter BCRP/ABCG2. *PLoS ONE, 7*(2). doi:10.1371/journal.pone.0030456

Hyndman, D., Liu, S., & Miner, J. N. (2016). Urate Handling in the Human Body. *Current Rheumatology Reports, 18*(6). doi:10.1007/s11926-016-0587-7

Jay, G. D., Elsaid, K. A., Kelly, K. A., Anderson, S. C., Zhang, L., Teeple, E., Waller, K., & Fleming, B. C. (2012). Prevention of cartilage degeneration and gait asymmetry by lubricin tribosupplementation in the

rat following anterior cruciate ligament transection. *Arthritis and rheumatism*, *64*(4), 1162–1171. https://doi.org/10.1002/art.33461

Jay, G. D., & Waller, K. A. (2014). The biology of Lubricin: Near frictionless joint motion. *Matrix Biology, 39*, 17-24. doi:10.1016/j.matbio.2014.08.008

Lakes, E. H., & Allen, K. D. (2016). Gait analysis methods for rodent models of arthritic disorders: reviews and recommendations. *Osteoarthritis and cartilage*, *24*(11), 1837–1849. https://doi.org/10.1016/j.joca.2016.03.008

Lu, J., Hou, X., Yuan, X., Cui, L., Liu, Z., Li, X., Ma, L., Cheng, X., Xin, Y., Wang, C., Zhang, K., Wang, X., Ren, W., Sun, R., Jia, Z., Tian, Z., Mi, Q. S., & Li, C. (2018). Knockout of the urate oxidase gene provides a stable mouse model of hyperuricemia associated with metabolic disorders. *Kidney international*, *93*(1), 69–80. https://doi.org/10.1016/j.kint.2017.04.031

Marcelino, J., Carpten, J. D., Suwairi, W. M., Gutierrez, O. M., Schwartz, S., Robbins, C., Sood, R., Makalowska, I., Baxevanis, A., Johnstone, B., Laxer, R. M., Zemel, L., Kim, C. A., Herd, J. K., Ihle, J., Williams, C., Johnson, M., Raman, V., Alonso, L. G., Brunoni, D., … Warman, M. L. (1999). CACP, encoding a secreted proteoglycan, is mutated in camptodactyly-arthropathy-coxa vara-pericarditis syndrome. *Nature genetics*, *23*(3), 319–322. https://doi.org/10.1038/15496

Martillo, M. A., Nazzal, L., & Crittenden, D. B. (2013). The Crystallization of Monosodium Urate. *Current Rheumatology Reports, 16*(2). doi:10.1007/s11926-013-0400-9

Parathithasan, N., Lee, W. K., Pianta, M., Oon, S., & Perera, W. (2016). Gouty arthropathy: Review of clinico-pathologic and imaging features. *Journal of medical imaging and radiation oncology*, *60*(1), 9–20. https://doi.org/10.1111/1754-9485.12356

Plaas, A., Li, J., Riesco, J., Das, R., Sandy, J. D., & Harrison, A. (2011). Intraarticular injection of hyaluronan prevents cartilage erosion, periarticular fibrosis and mechanical allodynia and normalizes stance time in murine knee osteoarthritis. *Arthritis research & therapy*, *13*(2), R46. https://doi.org/10.1186/ar3286

Qadri, M., Schmidt, T., Elsaid, K., Jay, G. (2016, September 28). *Recombinant human proteoglycan-4 (RHPRG4) inhibits monosodium urate (MSU) crystal phagocytosis by human macrophages and resultant*

inflammatory response. ACR Meeting Abstracts. Retrieved November 7, 2021, from https://acrabstracts.org/abstract/recombinant-human-proteoglycan-4-rhprg4-inhibits-monosodium-urate-msu-crystal-phagocytosis-by-human-macrophages-and-resultant-inflammatory-response/.

Qadri, M., Jay, G. D., Zhang, L. X., Wong, W., Reginato, A. M., Sun, C., . . . Elsaid, K. A. (2018). Recombinant human proteoglycan-4 reduces phagocytosis of urate crystals and downstream nuclear factor kappa B and inflammasome activation and production of cytokines and chemokines in human and murine macrophages. *Arthritis Research & Therapy, 20*(1). doi:10.1186/s13075-018-1693-x

Ragab, G., Elshahaly, M., & Bardin, T. (2017). Gout: An old disease in new perspective – A review. *Journal of Advanced Research, 8*(5), 495-511. doi:10.1016/j.jare.2017.04.008

Rai, S. K., Burns, L. C., De Vera, M. A., Haji, A., Giustini, D., & Choi, H. K. (2015). The economic burden of gout: A systematic review. *Seminars in arthritis and rheumatism, 45*(1), 75–80. https://doi.org/10.1016/j.semarthrit.2015.02.004

Reginato, AM., Qadri, M., Sun, C., Schmidt, T., Yang, N., Elsaid, K., Jay, G. (2016) Anti-Inflammatory Role of Lubricin/Proteoglycan 4 (PRG4) in Monosodium Urate (MSU)-Crystal Induced Arthritis. [abstract]. *Arthritis Rheumatol, 68 (suppl 10).* https://acrabstracts.org/abstract/anti-inflammatory-role-of-lubricinproteoglycan-4-prg4-in-monosodium-urate-msu-crystal-induced-arthritis/.

Schlesinger N. (2014). Anti-interleukin-1 therapy in the management of gout. Current rheumatology reports, 16(2), 398. https://doi.org/10.1007/s11926-013-0398-z

Singh J. A. (2013). Racial and gender disparities among patients with gout. *Current rheumatology reports, 15*(2), 307. https://doi.org/10.1007/s11926-012-0307-x

Towiwat, P., Chhana, A., & Dalbeth, N. (2019). The anatomical pathology of gout: A systematic literature review. *BMC Musculoskeletal Disorders, 20*(1). doi:10.1186/s12891-019-2519-y

U.S. Department of Health and Human Services. (n.d.). *AVMA guidelines for the euthanasia of animals: 2020 edition posted*. National Institutes of Health. Retrieved November 30, 2021, from https://olaw.nih.gov/news/avma-guidelines-euthanasia-animals-2020-edition-posted.html.

Vugmeyster, Y., Wang, Q., Xu, X., Harrold, J., Daugusta, D., Li, J., Zollner, R., Flannery, C. R., & Rivera-Bermúdez, M. A. (2012). Disposition of human recombinant lubricin in naive rats and in a rat model of post-traumatic arthritis after intra-articular or intravenous administration. *The AAPS journal*, *14*(1), 97–104. https://doi.org/10.1208/s12248-011-9315-4

Waller, K. A., Zhang, L. X., Elsaid, K. A., Fleming, B. C., Warman, M. L., & Jay, G. D. (2013). Role of lubricin and boundary lubrication in the prevention of chondrocyte apoptosis. *Proceedings of the National Academy of Sciences, 110*(15), 5852-5857. doi:10.1073/pnas.1219289110

Wilson, N., Kariisa, M., Seth, P., Smith, H., 4th, & Davis, N. L. (2020). Drug and Opioid-Involved Overdose Deaths - United States, 2017-2018. *MMWR. Morbidity and mortality weekly report*, *69*(11), 290–297. https://doi.org/10.15585/mmwr.mm6911a4

Appendix 1

Exemplar Raw DigiGait Data: IA MSU crystal Injection in *Prg4* Conditional Mice Gait Analysis

The raw DigiGait data export for the Pre-Injection data sample is included below, one animal for test group:

Table 20. Pre-Injection data													
FileName		control				pbs				tam			
Limb		Left Fore	Right Fore	Left Hind	Right Hind	Left Fore	Right Fore	Left Hind	Right Hind	Left Fore	Right Fore	Left Hind	Right Hind
Swing	(s)	0.137	0.121	0.115	0.084	0.086	0.107	0.093	0.087	0.1	0.134	0.108	0.071
%SwingStride	(%)	42.1	37.4	34.2	37	38.4	45.9	38.7	35	29.9	39.4	31.2	27.8
Brake	(s)	0.082	0.103	0.063	0.079	0.082	0.082	0.031	0.043	0.14	0.118	0.038	0.038
%BrakeStride	(%)	25.4	31.9	18.6	35.1	36.5	35.3	13	17.3	41.9	34.6	11.1	14.8
Propel	(s)	0.105	0.099	0.159	0.063	0.056	0.044	0.116	0.118	0.095	0.089	0.2	0.147
%PropelStride	(%)	32.4	30.7	47.2	27.9	25.2	18.8	48.4	47.7	28.2	26	57.7	57.3
Stance	(s)	0.188	0.202	0.221	0.142	0.138	0.126	0.147	0.161	0.235	0.206	0.238	0.185
%StanceStride	(%)	57.9	62.6	65.8	63	61.6	54.1	61.3	65	70.1	60.6	68.8	72.2
Stride	(s)	0.324	0.323	0.336	0.226	0.224	0.233	0.24	0.248	0.335	0.34	0.346	0.256
%BrakeStance	(%)	43.9	51	28.3	55.7	59.2	65.3	21.1	26.6	59.7	57.1	16.1	20.5
%PropelStance	(%)	56.1	49	71.7	44.3	40.8	34.7	78.9	73.4	40.3	42.9	83.9	79.5
Stance/Swing	(real#)	1.4	1.7	1.9	1.7	1.6	1.2	1.6	1.9	2.3	1.5	2.2	2.6
StrideLength	(cm)	5.5	5.5	5.7	3.8	6.3	6.5	6.7	6.9	4.4	4.4	4.5	3.3
Stride Frequency	(steps/s)	3.1	3.1	3	4.3	4.4	4.2	4.3	4	3	2.9	3	4

PawAngle	(deg)	-11.9	6.6	-13.8	11.1	-8.7	-0.9	-19.1	12.9	-6.5	7.3	-16.1	20.9
Absolute PawAngle	(deg)	11.9	6.6	13.8	11.1	8.7	0.9	19.1	12.9	6.5	7.3	16.1	20.9
Paw Angle Variability	(deg)	6.6	13.9	3	15.8	13.9	16.8	4.2	10.8	4.8	5.9	10.2	7.8
StanceWidth	(cm)	1.6	-	2.8	-	1.9	-	2.5	-	1.6	-	3.1	-
StepAngle	(deg)	67.1	-	59.7	-	58.5	-	52.4	-	62.2	-	57.3	-
SLVar	(cm)	2.12	1.13	1.28	1.6	1.51	1.03	0.82	0.69	1.45	2.02	1.77	1.59
SWVar	(cm)	0.73	-	0.16	-	0.28	-	0.22	-	0.64	-	0.43	-
StepAngleVar	(deg)	17.36	-	22.25	-	19.59	-	7.35	-	21.21	-	20.58	-
#Steps	(real#)	10.5	9	11	7	9	7.5	10	11	11.5	12.5	12.5	16
Stride Length CV	(CV%)	38.45	20.51	22.32	41.68	24.05	15.79	12.22	10.01	33.18	45.61	39.35	47.76
Stance Width CV	(CV%)	45.97	-	5.84	-	15.12	-	8.76	-	41.33	-	13.98	-
Step Angle CV	(CV%)	25.87	-	37.3	-	33.45	-	14.02	-	34.1	-	35.88	-
Swing Duration CV	(CV%)	37.21	36.37	30.5	66.5	33.5	14.18	12.75	16.91	55.68	44.22	45.67	60.41
Paw Area at Peak Stance in sq. cm	(cm^2)	0.25	0.22	0.48	0.15	0.39	0.32	0.71	0.59	0.28	0.28	0.49	0.37
Paw Area Variability at Peak Stance in sq. cm	(cm^2)	0.03	0.02	0.02	0.07	0.03	0.04	0.07	0.07	0.02	0.02	0.06	0.09
Hind Limb Shared Stance Time	(s)	-	-	0.109	-	-	-	0.059	-	-	-	0.141	-
% Shared Stance	(%)	-	-	49.1	76.6	-	-	39.8	36.3	-	-	59.3	76.6
StanceFactor	(real#)	0.93	-	1.56	-	1.1	-	0.91	-	1.14	-	1.29	-

Gait Symmetry	(real#)	0.85	0.85	0.85	0.85	1.04	1.04	1.04	1.04	0.86	0.86	0.86	0.86
MAX dA/dT	(cm^2/s)	19	17.67	42.8	9.14	27.51	21.36	69.64	54.8	23.57	19.83	50.42	36.64
MIN dA/dT	(cm^2/s)	-5.81	-7.72	-9.3	-7.41	-13.1	-11.57	-19.77	-16.17	-8.19	-10.34	-10.59	-11.36
Tau - Propulsion	(real#)	-	-	0.1073	0.0733	-	-	0.0519	0.0486	-	-	0.0961	0.0661
Overlap Distance	(cm)	1.86	2.9	1.86	2.9	-0.15	-2.7	-0.15	-2.7	2	2.13	2	2.13
PawPlacementPositioning[PPP]	(cm)	0.69	0.95	0.69	0.95	0.37	0.15	0.37	0.15	0.57	0.75	0.57	0.75
Ataxia Coefficient	(real#)	1.35	0.68	0.84	1.1	0.61	0.43	0.42	0.29	1.01	1.56	1.44	1.74
Midline Distance	(cm)	-2.86	-2.62	1.57	2.29	-2.59	-2.48	1.49	1.73	-2.56	-2.45	1.81	1.07
Axis Distance	(cm)	-0.9	0.75	-1.3	1.46	-0.81	0.98	-1.19	1.57	-0.93	0.84	-1.47	1.53
Paw Drag	(real#)	-	-	1.066	0.012	-	-	-0.851	-0.437	-	-	-0.623	-0.171
Belt Speed	(cm/s)	17	17	17	17	28	28	28	28	13	13	13	13
User Name		Optional	Optional	Optional	Optional	Optional	Optional	Optional	Optional	Optional	Optional	Optional	Optional

The raw DigiGait data export for the Post-Injection data sample is included below, one animal for test group:

Table 21. Post-Injection data													
FileName		control				pbs				tam			
Limb		Left Fore	Right Fore	Left Hind	Right Hind	Left Fore	Right Fore	Left Hind	Right Hind	Left Fore	Right Fore	Left Hind	Right Hind
Swing	(s)	0.098	0.056	0.075	0.048	0.049	0.063	0.042	0.04	0.062	0.073	0.051	0.053

%SwingStride	(%)	41	43.3	32.5	27.6	37	48	39.9	39	30.5	32.7	35.2	46.4
Brake	(s)	0.053	0.033	0.048	0.033	0.051	0.038	0.011	0.011	0.061	0.108	0.04	0.022
%BrakeStride	(%)	22	25.6	20.9	18.6	38.2	29	10.5	10.4	30.1	48.4	28	18.9
Propel	(s)	0.089	0.04	0.108	0.094	0.033	0.03	0.053	0.052	0.08	0.042	0.053	0.04
%PropelStride	(%)	37	31.1	46.6	53.8	24.8	23	49.7	50.6	39.4	18.9	36.8	34.7
Stance	(s)	0.142	0.073	0.156	0.127	0.083	0.069	0.064	0.062	0.142	0.151	0.093	0.061
%StanceStride	(%)	59	56.7	67.5	72.4	63	52	60.1	61	69.5	67.3	64.8	53.6
Stride	(s)	0.24	0.129	0.231	0.176	0.133	0.132	0.106	0.102	0.204	0.224	0.144	0.114
%BrakeStance	(%)	37.2	45.2	30.9	25.7	60.6	55.8	17.4	17	43.3	72	43.2	35.3
%PropelStance	(%)	62.8	54.8	69.1	74.3	39.4	44.2	82.6	83	56.7	28	56.8	64.7
Stance/Swing	(real#)	1.4	1.3	2.1	2.6	1.7	1.1	1.5	1.6	2.3	2.1	1.8	1.2
StrideLength	(cm)	6	3.2	5.8	4.4	3.5	3.4	2.8	2.7	1.6	1.8	1.2	0.9
Stride Frequency	(steps/s)	4.2	8	4.4	5.9	7.8	7.8	9.9	10.2	5	4.5	7.2	9.1
PawAngle	(deg)	-3.6	6.9	-9.2	10.9	0	1.4	-15.8	9.7	-8.7	11.6	-10.2	19.3
Absolute PawAngle	(deg)	3.6	6.9	9.2	10.9	0	1.4	15.8	9.7	8.7	11.6	10.2	19.3
Paw Angle Variability	(deg)	5.4	11.7	3.6	4.6	20.6	15	8.6	25.3	6.3	20.2	13.9	19.8
StanceWidth	(cm)	1.8	-	2.8	-	2	-	2.9	-	1.6	-	2.2	-
StepAngle	(deg)	72.7	-	52.8	-	56.4	-	37.1	-	56.2	-	46.1	-
SLVar	(cm)	1.52	1.6	2.34	2.25	2.22	1.95	1.92	1.25	0.98	1.44	0.71	0.61
SWVar	(cm)	0.62	-	0.22	-	0.81	-	0.8	-	0.92	-	0.93	-
StepAngleVar	(deg)	21.96	-	17.14	-	17.59	-	20.92	-	24.29	-	24.5	-
#Steps	(real#)	6.5	22	9.5	17	20.5	20.5	15	27.5	15	13	13	30.5

Stride Length CV	(CV%)	25.32	49.74	40.6	51.33	64.09	56.75	69.71	46.9	60.26	80.56	61.26	67.29
Stance Width CV	(CV%)	35.18	-	7.86	-	39.82	-	27.86	-	58.35	-	42.17	-
Step Angle CV	(CV%)	30.2	-	32.46	-	31.21	-	56.38	-	43.24	-	53.16	-
Swing Duration CV	(CV%)	15.96	60.3	48.03	71.82	90.69	80.23	86.05	73.25	86.42	93.51	147.64	99.01
Paw Area at Peak Stance in sq. cm	(cm^2)	0.25	0.19	0.45	0.33	0.21	0.18	0.32	0.2	0.18	0.14	0.21	0.12
Paw Area Variability at Peak Stance in sq. cm	(cm^2)	0.01	0.04	0.08	0.12	0.1	0.06	0.07	0.1	0.05	0.05	0.04	0.07
Hind Limb Shared Stance Time	(s)	-	-	0.104	-	-	-	0.044	-	-	-	0.049	-
% Shared Stance	(%)	-	-	66.5	81.5	-	-	69	70.5	-	-	53	80.9
StanceFactor	(real#)	1.94	-	1.23	-	1.22	-	1.02	-	0.94	-	1.53	-
Gait Symmetry	(real#)	1.18	1.18	1.18	1.18	0.77	0.77	0.77	0.77	0.58	0.58	0.58	0.58
MAX dA/dT	(cm^2/s)	20.4	17.12	38.42	29.42	17.9	17.1	29.24	19.24	17	11.79	19.83	10.87
MIN dA/dT	(cm^2/s)	-5.03	-6.73	-14.35	-13.72	-14.7	-8.73	-25.31	-10.93	-7.44	-6.27	-11.13	-8.06
Tau - Propulsion	(real#)	-	-	0.0697	0.1556	-	-	0.049	0.0498	-	-	-0.1471	0.742
Overlap Distance	(cm)	-0.13	0.94	-0.13	0.94	1.01	1.28	1.01	1.28	2.38	2.46	2.38	2.46
PawPlacementPositioning[PPP]	(cm)	0.74	0.77	0.74	0.77	0.7	0.05	0.7	0.05	0.44	1.21	0.44	1.21
Ataxia Coefficient	(real#)	0.68	1.56	1.24	1.7	2.11	2.21	2.16	1.78	2.43	2.19	2.02	3.23

Midline Distance	(cm)	-3.87	-3.49	1.57	0.35	-1.15	-3.03	1.23	0.35	-2.48	-1.47	1.24	1.45
Axis Distance	(cm)	-0.78	0.68	-1.39	1.39	-1.14	0.75	-1.53	1.01	-1	0.7	-0.99	1.26
Paw Drag	(real#)	-	-	-0.596	-1.037	-	-	-2.533	-3.286	-	-	-2.057	-0.433
Belt Speed	(cm/s)	25	25	25	25	26.1	26.1	26.1	26.1	8	8	8	8
User Name		Optional	Optional	Optional	Optional	Optional	Optional	Optional	Optional	Optional	Optional	Optional	Optional

Appendix 2

DigiGait Mouse Analysis – IA HDV-Prg4 Injection in *Prg4* Null Mice

The same DigiGait metrics were assessed for the PRG4 Null Mice and are included below.

Figure 15.

HDV-PRG4 Injection in PRG4 Null Mice

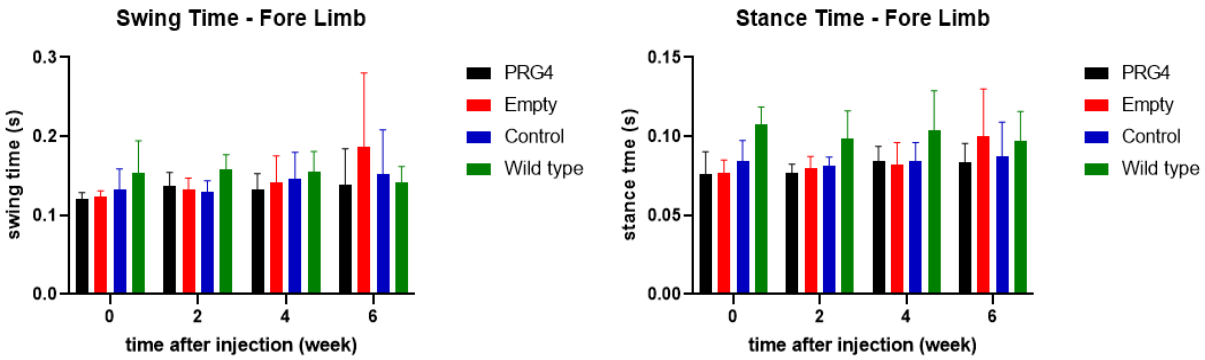

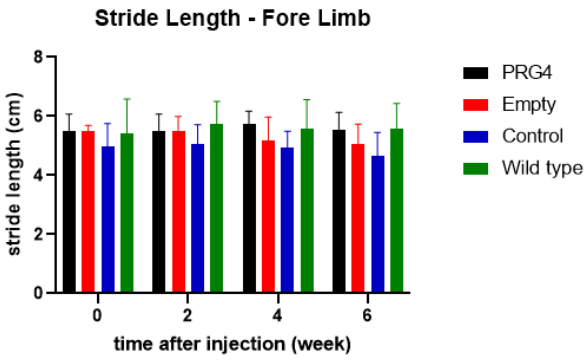

Legend: HDV-Prg4, HDV-empty, no HDV injection, and wild type animals showed that there were no consistent measurements of reversable gait differences between HDV-empty and HDV-Prg4 over time.

4 week old wild type, *Prg4*$^{-/-}$ mice that received the IA HDV-EF1-*Prg4*, HDV-empty injection, and no injection were assessed in gait analysis 0 weeks, 2 weeks, 4 weeks, and 6 weeks following the injection. These groups were selected to study if there would be reversable gait differences within the HDV-EFI-*Prg4* group compared to others. Based on this data, there are significant differences between the animal group performances and over time, specifically detailed in the tables below.

The differences between gait for each group were always more significant over time, typically within the 6 week group. In swing time, there was a noticeable difference between the *Prg4* (average 0.138s) and empty (average 0.186s) group at 6 weeks. This was also true for stance time, at 6 weeks there was a difference between the PRG4 group (average 0.083s) and the empty group (average 0.100s). It is also worth noting that the wild type gait data does not typically trend over time for any of the metrics, as was seen in the other groups.

Table 22. Swing Time, Test Group					
Tukey's multiple comparisons test	Predicted (LS) mean diff.	95% CI of diff.	Below threshold?	Summary	Adjusted P Value
6 weeks					

PRG4 vs. Empty	-0.04795	-0.08706 to -0.008846	Yes	**	0.0094

Table 23. Swing Time, Time Groups					
Tukey's multiple comparisons test	Predicted (LS) mean diff.	95% CI of diff.	Below threshold?	Summary	Adjusted P Value
Empty					
0 vs. 6 weeks	-0.06285	-0.1007 to -0.02496	Yes	***	0.0002
2 vs. 6 weeks	-0.05372	-0.09161 to -0.01582	Yes	**	0.0018
4 vs. 6 weeks	-0.04377	-0.08361 to -0.003920	Yes	*	0.0251

Table 24. Stance Time, Test Group					
Tukey's multiple comparisons test	Predicted (LS) mean diff.	95% CI of diff.	Below threshold?	Summary	Adjusted P Value
0 weeks					
PRG4 vs. Wild type	-0.03137	-0.05305 to -0.009688	Yes	**	0.0014
Empty vs. Wild type	-0.03100	-0.05012 to -0.01188	Yes	***	0.0003
Control vs. Wild type	-0.02372	-0.04343 to -0.004005	Yes	*	0.0113
2 weeks					
PRG4 vs. Wild type	-0.02140	-0.04024 to -0.002560	Yes	*	0.0190
4 weeks					
PRG4 vs. Wild type	-0.01956	-0.03885 to -0.0002643	Yes	*	0.0456
Empty vs. Wild type	-0.02187	-0.04158 to -0.002155	Yes	*	0.0232
6 weeks					

PRG4 vs. Empty	-0.01689	-0.03206 to -0.001717	Yes	*	0.0226

Table 25. Stance Time, Time Groups					
Tukey's multiple comparisons test	Predicted (LS) mean diff.	95% CI of diff.	Below threshold?	Summary	Adjusted P Value
Empty					
0 vs. 6 weeks	-0.02347	-0.03817 to -0.008773	Yes	***	0.0003
2 vs. 6 weeks	-0.02027	-0.03497 to -0.005573	Yes	**	0.0026
4 vs. 6 weeks	-0.01794	-0.03340 to -0.002482	Yes	*	0.0158

Table 26. Stride Length Test Group					
Tukey's multiple comparisons test	Predicted (LS) mean diff.	95% CI of diff.	Below threshold?	Summary	Adjusted P Value
4 weeks					
PRG4 vs. Control	0.7917	0.1313 to 1.452	Yes	*	0.0117
6 weeks					
PRG4 vs. Control	0.8635	0.1915 to 1.535	Yes	**	0.0058
Control vs. Wild type	-0.9050	-1.799 to -0.01148	Yes	*	0.0459

Figure 16.

Graphical data of all metrics for the HDV-Prg4 mice gait

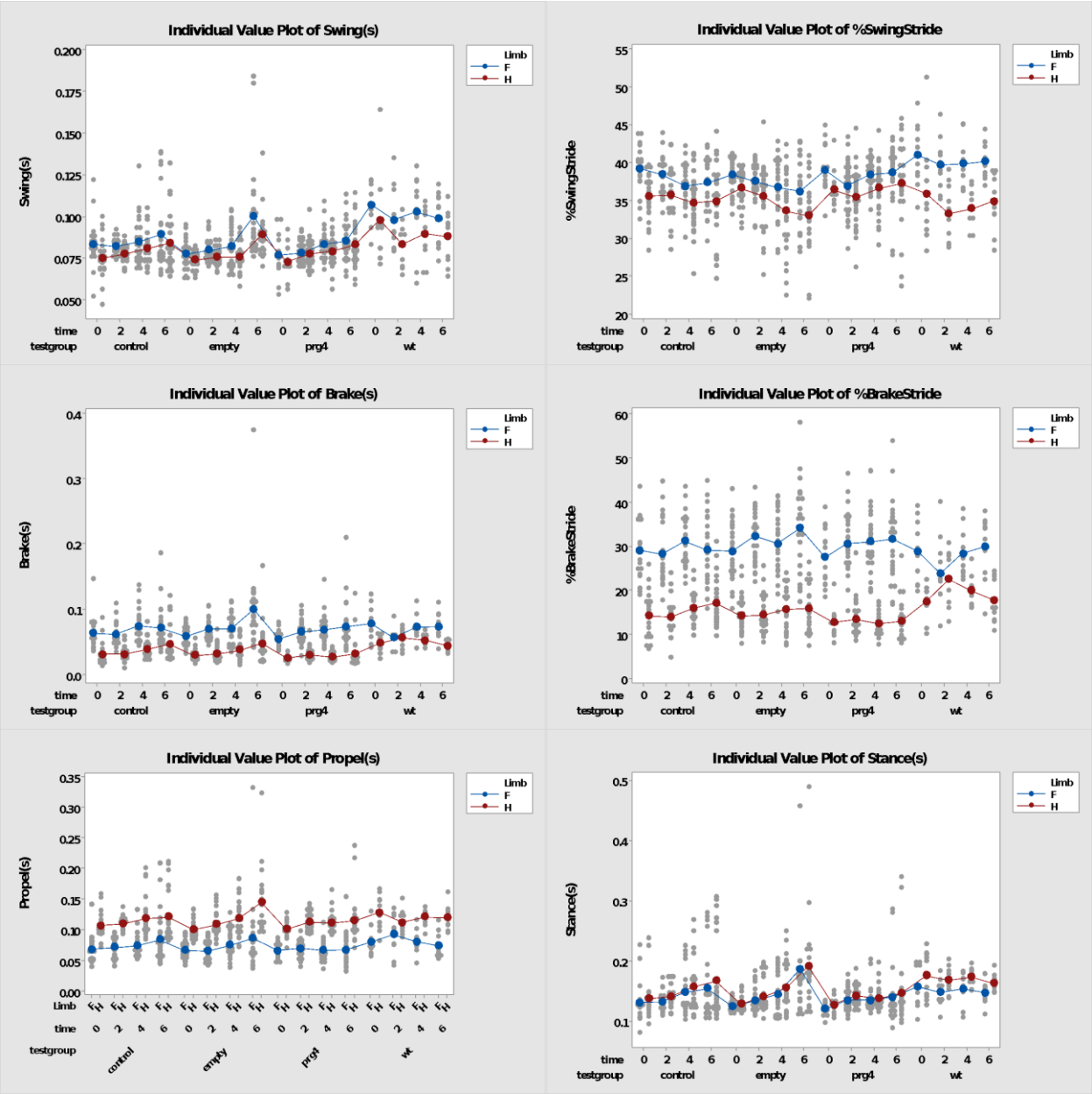

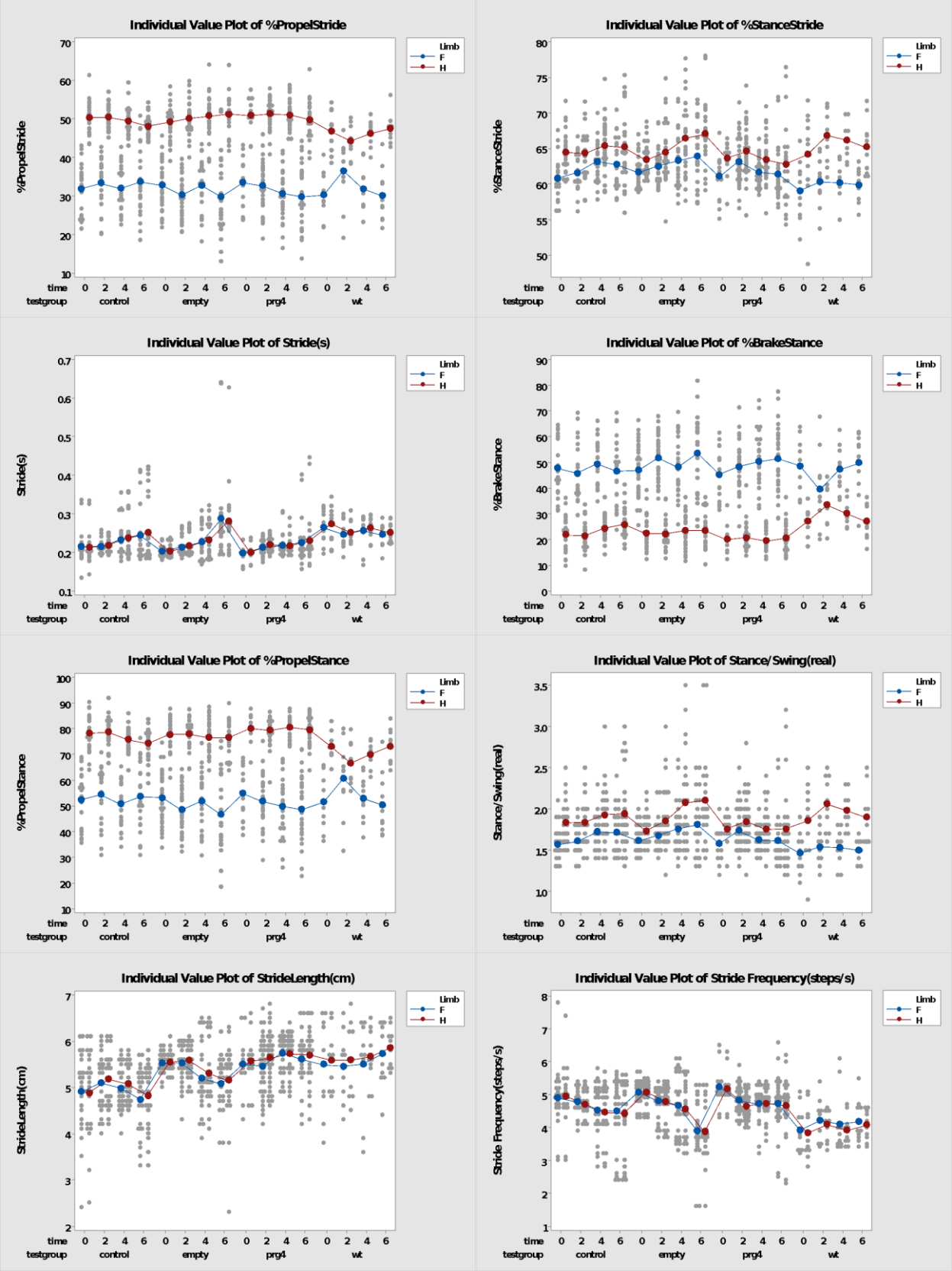
Individual Value Plot of %PropelStride
%PropelStride
Individual Value Plot of %StanceStride
%StanceStride
Individual Value Plot of Stride(s)
Stride(s)
Individual Value Plot of %BrakeStance
%BrakeStance
Individual Value Plot of %PropelStance
%PropelStance
Individual Value Plot of Stance/Swing(real)
Stance/Swing(real)
Individual Value Plot of StrideLength(cm)
StrideLength(cm)
Individual Value Plot of Stride Frequency(steps/s)
Stride Frequency(steps/s)
Limb
F
H
time
testgroup
control
empty
prg4
wt

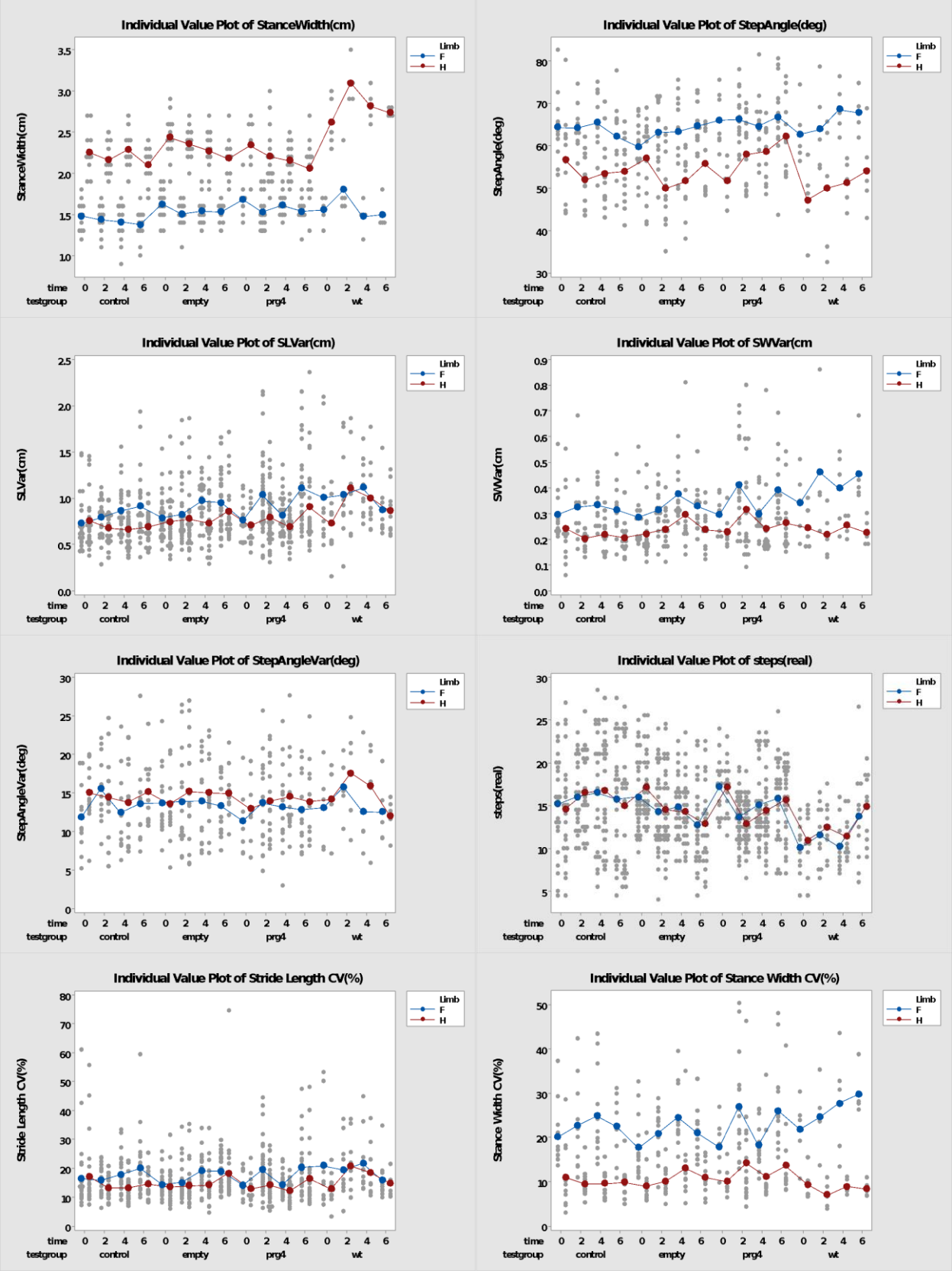
Individual Value Plot of StanceWidth(cm)
StanceWidth(cm)
Individual Value Plot of StepAngle(deg)
StepAngle(deg)
Individual Value Plot of SLVar(cm)
SLVar(cm)
Individual Value Plot of SWVar(cm
SWVar(cm
Individual Value Plot of StepAngleVar(deg)
StepAngleVar(deg)
Individual Value Plot of steps(real)
steps(real)
Individual Value Plot of Stride Length CV(%)
Stride Length CV(%)
Individual Value Plot of Stance Width CV(%)
Stance Width CV(%)
Limb
F
H
time
testgroup
control
empty
prg4
wt

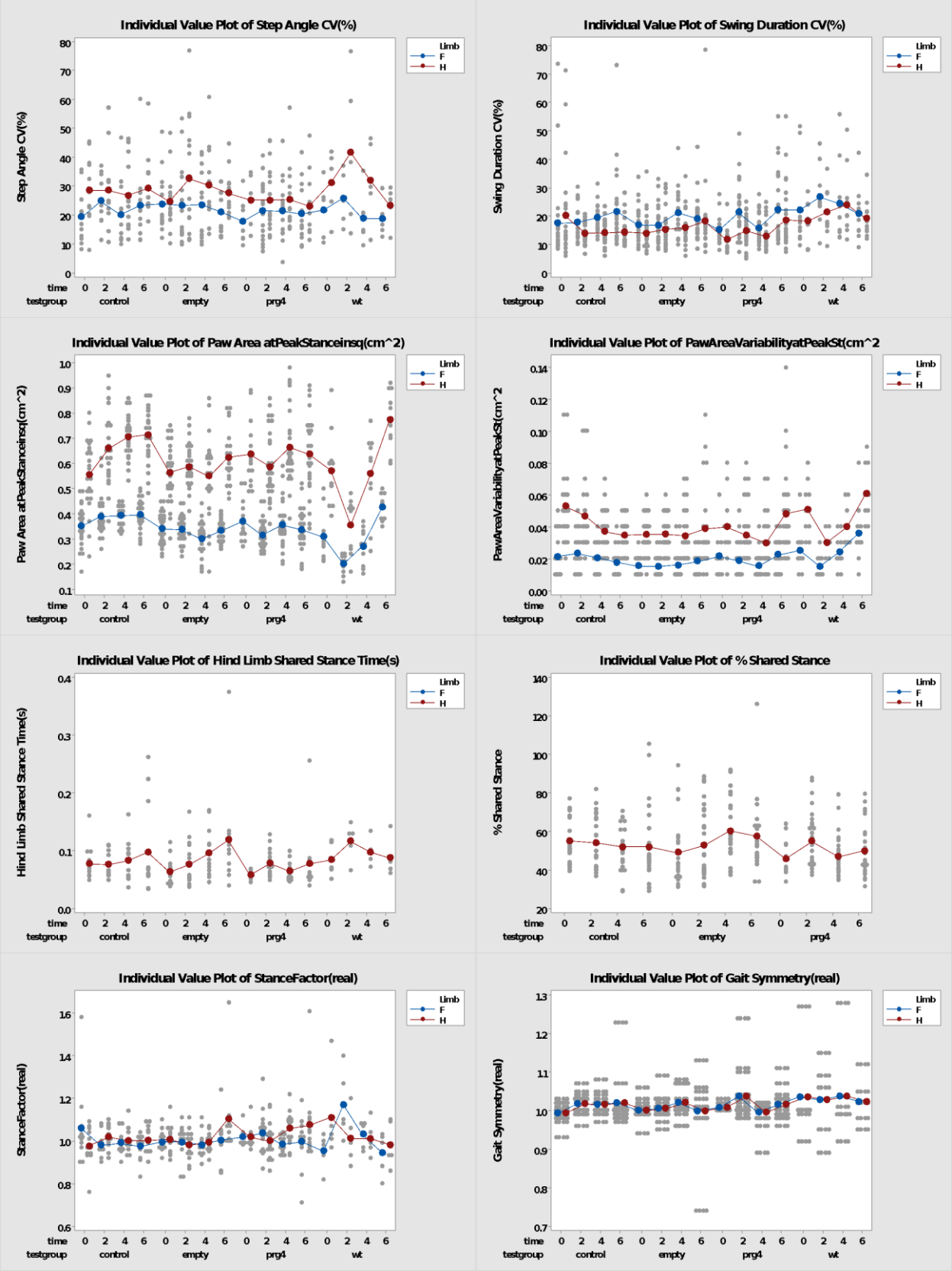
Individual Value Plot of Step Angle CV(%)
Step Angle CV(%)
Individual Value Plot of Swing Duration CV(%)
Swing Duration CV(%)
Individual Value Plot of Paw Area atPeakStanceinsq(cm^2)
Paw Area atPeakStanceinsq(cm^2)
Individual Value Plot of PawAreaVariabilityatPeakSt(cm^2
PawAreaVariabilityatPeakSt(cm^2
Individual Value Plot of Hind Limb Shared Stance Time(s)
Hind Limb Shared Stance Time(s)
Individual Value Plot of % Shared Stance
% Shared Stance
Individual Value Plot of StanceFactor(real)
StanceFactor(real)
Individual Value Plot of Gait Symmetry(real)
Gait Symmetry(real)
Limb
F
H
time
testgroup
control
empty
prg4
wt

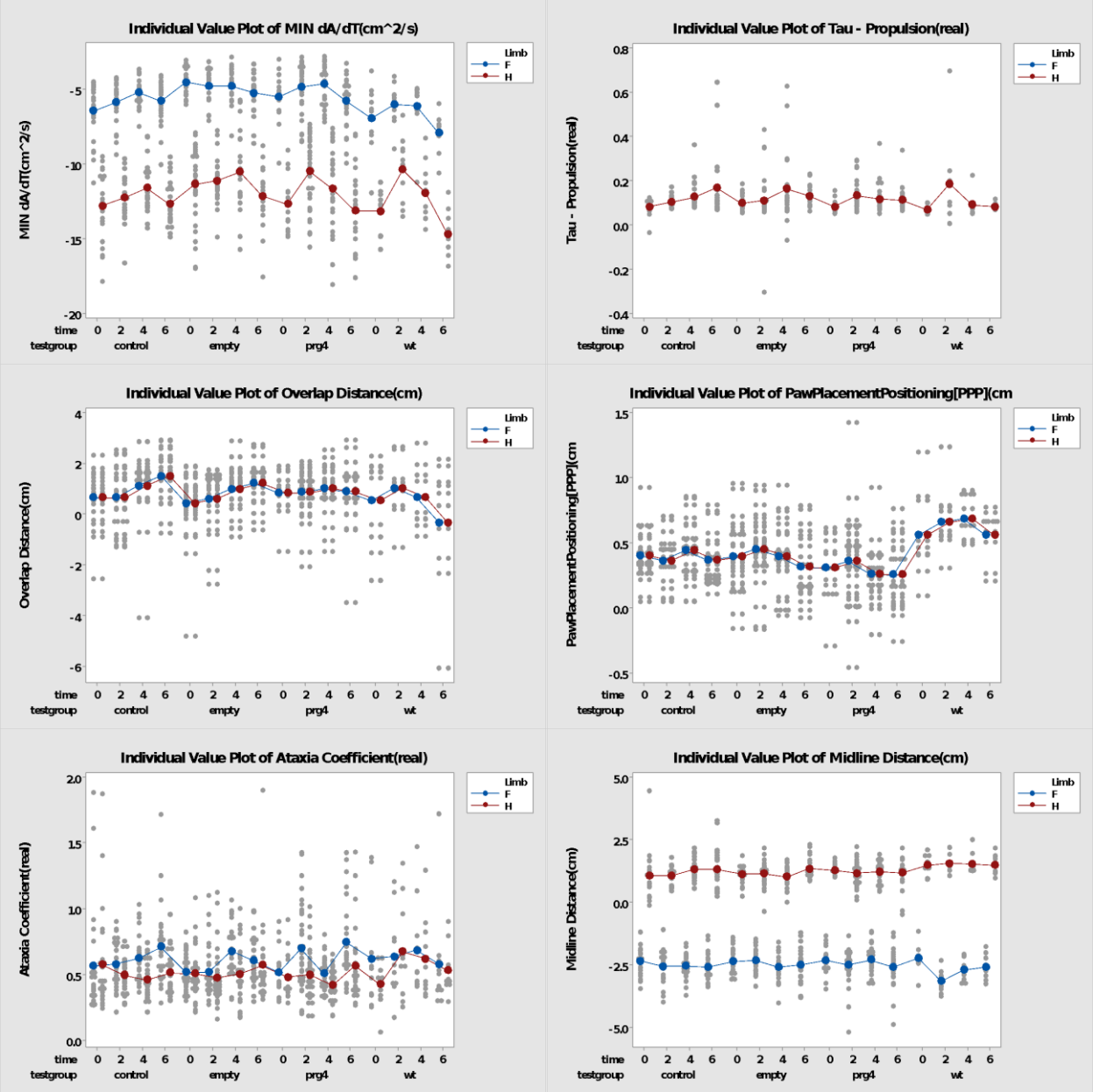

Legend: HDV-EF1-Prg4, HDV-EF1-empty, no HDV injection, and wild type animals showed that there were no consistent measurements of reversable gait differences between HDV-EF1-empty and HDV-EF1-Prg4 over time.

Appendix 3

Methods: *Prg4*$^{-/-}$ Joint Friction Data study

1. Outline: 4-week-old *Prg4*$^{-/-}$ mice were injected with tamoxifen, corn oil, or received no injection, then 10 weeks later were euthanized to evaluate for knee joint friction using the Qualisys system, including wild type animals of the same age.
2. Relevance: This study provides joint friction data assessing the effect of *Prg4*$^{-/-}$ with and without lubricin expression and compared to wild type animals.

Method Specific Protocol: *Prg4*$^{-/-}$ Joint Friction Data *study ongoing*

1. Mice Preparation

Prg4$^{-/-}$ male and female mice were injected in their hind limbs with tamoxifen, corn oil, or no injection then euthanized 10 weeks later. Wild type animals were also included in this study.

2. Mice Dissection

The mice were euthanized, and the left and right knee joints were dissected. Using scissors, the skin and fur was cut away from the hindlimb to expose the joint. The hindlimb was separated from the body by cutting through the muscles and hip joint, then the foot was just away at the ankle. The soft tissue was dissected off the bottom of the femur and tibia. The muscle and remaining tissue were trimmed around the joint capsule and kept wrapped in saline-soaked gauze until testing.

3. Specimen preparation

Square Brass tubes ¼" (McMaster-Carr: Part# 8859K46; www.mcmaster.com) width were cut to be 1" long, with two tubes required per knee joint. Using clay, the brass tubes were arranged to hold the joint so that it can flex and then capped at the ends with the clay. Smooth-cast urethane compound (Smooth Cast 300Q; http://www.smooth-on.com/Urethane-Plastic-a/cs_1120_1209/index.htmI) was mixed together and

added to the brass tubes to encase the joint. This was allowed to fully try until testing, with soaked gauze covering the joint.

4. Data collection Preparation

Qualisys DHCP was used to perform the knee joint friction measurements. The four collection cameras were arranged to have a direct view of the knee joint at the desired location of testing. They were connected in series, with the master camera the initial connection to the computer. Once connected and powered, the Qualisys DHCP and Track manager software was opened. The view of the cameras was confirmed with the Qualisys collection and masks were applied as needed. The system was calibrated by removing and covering all markers on the pendulum and base. The L-frame was located on the base pendulum, and the wand was waved to mimic the pendulum area of measurement during calibration. A standing and oscillation file was collected in preparation to confirm the set up. An aim model was created to locate the identification markers, and applied for each data test run.

5. Pendulum Mounting

The top of the femur tube was inserted into the notch of the pendulum, and the tibia tube was secured in the mounting block. Cell culture media was added to the mounting block so that the knee joint was partially submerged during testing.

6. File collection & Export

Standing and N=3 oscillation files at t=7min apart were collected for each joint until the swinging fully stopped. The data was saved and exported at each file collection. All data was batched and exported to C3D format (.c3d files) and saved for final processing and analysis.